CONTAINMENT INTERNAL STRUCTURE: STIFFNESS AND DAMPING FOR ANALYSIS

MUAP-11018
Revision 1

Non-proprietary version

February 2013

© 2013 Mitsubishi Heavy Industries, Ltd.
All Rights Reserved

Revision History

Revision	Pages	Description
0	All	Initial Issue
1	vii-ix, 1-1, 2-10, Section 3 4-1, 4-2, 4-7, 4-8, 4-16, 5-1, 5-3, Section 6, 8-3; 9-1, 10-1,10-2 Appendices G, H, and J	Revision to incorporate responses to RAI 894-6270 Question 03.08.03-63 and RAI 905-6311 Question 03.08.03-72. Added discussion on the effect of stainless steel cladding on SC stiffness in Section 4.1.8 and in new Appendix G; added discussion of RC and SC stiffness comparison vs. reinforcement ratio in Section 8.3 and new Appendix H. Renamed previous Appendices G and H to Appendices I and K, respectively. Updated reference to ACI 349-01 with reference to ACI 349-06, and reference to MUAP-11001 with reference to MUAP-10006. Incorporated discussion of revised Accident Thermal loading. Discussion added to Abstract, Executive Summary, Section 3.3.2, Section 6.1, and Summary. Added Appendix J to compare previous vs. revised Accident Temperature vs. Time plots. Inserted new Figure 3-4 and 3-5 to illustrate temperatures in various compartments under thermal loading.

© 2013
MITSUBISHI HEAVY INDUSTRIES, LTD.
All Rights Reserved

This document has been prepared by Mitsubishi Heavy Industries, Ltd. (MHI) in connection with the United. States. Nuclear Regulatory Commission's (NRC) licensing review of MHI's US-APWR nuclear power plant design. No right to disclose, use or copy any of the information in this document, other that by the NRC and its contractors in support of the licensing review of the US-APWR, is authorized without the express written permission of MHI.

This document contains technology information and intellectual property relating to the US-APWR and it is delivered to the NRC on the express condition that it not be disclosed, copied or reproduced in whole or in part, or used for the benefit of anyone other than MHI without the express written permission of MHI, except as set forth in the previous paragraph.

This document is protected by the laws of Japan, U.S. copyright law, international treaties and conventions, and the applicable laws of any country where it is being used.

Mitsubishi Heavy Industries, Ltd.
16-5, Konan 2-chome, Minato-ku
Tokyo 108-8215 Japan

TABLE OF CONTENTS

LIST OF ACRONYMS

The following list defines the acronyms used in this document.

3-D	Three-Dimensional
ACI	American Concrete Institute
ASCE	American Society of Civil Engineers
CIS	Containment Internal Structure
FE	Finite Element
ISRS	In-Structure Response Spectra
LOCA	Loss of Coolant Accident
LEFE	Linear Elastic Finite Element
NRC	Nuclear Regulatory Commission
OBE	Operating-Basis Earthquake
PCCV	Prestressed Concrete Containment Vessel
R/B	Reactor Building
RC	Reinforced Concrete
RCL	Reactor Coolant Loop
RWSP	Refueling Water Storage Pit
SC	Steel Concrete
SG	Steam Generator
SRSS	Square Root Sum of The Squares
SSE	Safe-Shutdown Earthquake
SSI	Soil-Structure Interaction
TeR	Technical Report

LIST OF FIGURES

LIST OF TABLES

ABSTRACT

This Technical Report (TeR) presents the development of appropriate structural stiffness and damping values for the Containment Internal Structure (CIS) of the US-APWR standard plant. These stiffness and damping values will be used for modeling the dynamic behavior of the CIS while conducting: (i) Soil-Structure Interaction (SSI) analysis of the Reactor Building (R/B) complex, and (ii) subsequent structural analysis for calculating design force demands.

This TeR develops two sets of stiffness and damping values that are intended to capture the potential range of stresses and associated cracking levels in each of the different concrete structure types (or categories) in the CIS, including various Reinforced Concrete (RC) structures and the Steel Concrete (SC) primary and secondary shielding walls. The first set of values, identified as Condition “A”, represents the limited concrete cracking and higher stiffness anticipated for seismic loading during normal plant operations. The second set of values, identified as Condition “B”, represents the significant reduction in stiffness associated with extensive concrete cracking under seismic loading coupled with accident thermal conditions. The category-specific stiffness and damping values identified for each of these two conditions are based upon stress levels calculated in the basic design analyses. Appropriate values for the extent of cracking indicated by these stress levels are assigned to the RC structures (and other structures deemed to behave like RC) in accordance with available codes and regulatory guidance. The values assigned to the SC structures are based on experimentally verified stiffnesses that are similar in magnitude to those codified for RC structures, with small variations that are directly attributable to experimentally observed differences in SC behavior.

The transient thermal hydraulic analyses that generate the design accident thermal conditions for the CIS compartments have been revised. The Condition “B” stiffness terms presented in this TeR were based upon the original thermal hydraulic analyses. The present Revision of this TeR evaluates the differences between the original compartment temperature conditions and the revised conditions, and presents the basis for retaining the original Condition “B” stiffness terms.

EXECUTIVE SUMMARY

The US-APWR CIS is a complex structure that includes six different structure categories: (1) SC composite walls with thickness less than or equal to **[ ]**, (2) SC-type walls with thickness greater than **[ ]**, (3) SC-type primary shield walls with three steel plates and thickness from **[ ]**, (4) RC slabs, (5) massive RC structures, and (6) steel structures with non-structural concrete filling.

As shown in the Figures presented in Chapter 2 of this TeR, a majority of the CIS consists of Category 1 SC walls. This category includes the **[ ]**-thick SC walls that comprise the walls of the Steam Generator (SG) compartments, the **[ ]**-thick walls forming the Pressurizer compartment, the **[ ]**-thick outer walls of the Refueling Water Storage Pit (RWSP), and the **[ ]** -thick walls that comprise a majority of the Refueling Cavity. Some relatively small portions of the CIS utilize thicker SC walls, such as the **[ ]**-thick walls used for a limited segment of the Refueling Cavity. The only walls thicker than **[ ]** are the primary shield walls, which enclose the reactor cavity and support the reactor vessel. The primary shield is an SC-type structure that is **[ ]** thick over the majority of its height and consists of three steel plates (one on each surface and one in the middle) and numerous transverse steel plates.

Structure Categories 4 and 5 utilize conventional RC construction. Category 4 consists primarily of three major floor slabs at intervals along the height of the CIS, with thickness varying from **[ ]** Category 5 consists of the massive concrete structures at the base of the CIS, which form the bottom of the refueling cavity and also provide vertical support to the steam generators and the reactor coolant pumps. Lastly, Category 6 involves some steel structures (e.g., floor grids) with plain (nonstructural) concrete infill for radiation shielding.

This TeR presents the approach for estimating the structural stiffness and damping values of the various structure categories of the CIS, and modeling them using Linear Elastic Finite Element (LEFE) models to determine: (i) the In-Structure Response Spectra (ISRS) for equipment design and qualification, and (ii) structural member force demands for design.

The stiffness and damping values are commensurate with the level of concrete cracking expected to occur in the various structure categories of the CIS. The extent of concrete cracking varies for each loading combination applicable to the CIS design. Two basic loading combinations dominate in terms of dynamic response: (A) seismic loading during normal operating conditions, and (B) seismic loading plus accident thermal loading. These are referred to as Condition “A” and Condition “B”, respectively.

This TeR presents the stiffness and damping values for each of the structure categories of the CIS while accounting for the extent of concrete cracking associated with these two fundamental loading conditions.

Since a majority of the CIS consists of SC walls, and since there are no accepted U.S. codes that define the stiffness of SC walls for use in dynamic response analysis, this TeR gives particular attention to their behavior. In general, the behavior of SC walls is similar to that of RC walls that are conventionally used in safety-related nuclear facilities. Both of these structure types consist of thick concrete sections reinforced by steel. As a result, the extent of concrete cracking and its influence on the stiffness and damping will also be similar. However, some aspects of SC specific behavior can cause slight deviations from RC behavior. For

example: (i) the SC steel plates provide additional in-plane shear stiffness due to their continuous nature. (ii) the bond between SC steel plates and concrete will be intermittent (discontinuous) at shear connector locations. (iii) the reinforcement ratios for SC walls are much higher (approximately 2-4%).

The behavior of SC walls subjected to in-plane and out-of-plane forces and thermal loading has been studied experimentally in Japan and the U.S. Based on these experimental evaluations, some SC specific equations have been developed to represent their in-plane shear and flexural stiffness before and after cracking. The development of these equations and their correlation with experimental data has been presented in detail in Appendices A through E of this TeR.

The manner in which the experimentally based SC stiffness terms are assigned to the US-APWR SC walls is discussed in Chapter 5 (for Condition A) and Chapter 6 (for Condition B). The approach presented seeks to assign reasonably accurate yet conservative stiffness terms for these structures.

For example, the Category 1 SC walls that comprise a majority of the CIS are assigned in-plane shear stiffness terms that are based on best estimates of the extent of cracking expected for the “A” and “B” loading conditions, yet also result in rational upper and lower bounds of effective in-plane shear stiffness. More specifically, the extent of cracking in these walls under Condition “A” is estimated using the wall in-plane shear forces obtained from LEFE analysis of the CIS under safe-shutdown seismic loading. Based on the limited extent of cracking demonstrated by this analysis, fully uncracked in-plane shear stiffness is assigned to the Category 1 SC walls for Condition “A”. This upper bound in-plane shear stiffness is in turn paired with “fully cracked” in-plane shear stiffness for the extensive cracking observed in testing of SC walls exposed to accident thermal loading. Section 5.0 and 6.0 of this report provide details for Conditions “A” and “B” for all CIS categories.

Importantly, the transient thermal hydraulic analyses that generate the design accident thermal conditions for the CIS have been revised since the preparation of Revision 0 of this TeR. Appendix J compares the previous and revised thermal transient conditions and evaluates their effects. Based on this initial evaluation it was assumed that the revised thermal conditions do not have a significant impact on the dynamic behavior of the CIS (ISRS and design loads). Therefore this TeR retains the Condition “B” stiffness assessments that considered the original accident thermal loading. This determination will be confirmed by the revised basic design analysis using the revised thermal loading input.

This TeR also includes comparisons of the stiffness values calculated using SC specific equations and those estimated using RC behavior. These comparisons are very important because they demonstrate that in spite of SC specific behavior, the deviations from RC behavior are quite small and easily justifiable. They also verify the adequacy of using RC wall stiffness equations published in American Society of Civil Engineers (ASCE) 43-05 (Reference 1) for SC walls specific to the US-APWR CIS. The US-APWR project chose to use the SC specific stiffness and damping values for the Category 1 walls because they capture SC wall behavior more appropriately and are experimentally verified for the range of material and geometric parameters in use.

The table provided below summarizes the SC specific stiffness equations for the Category 1 SC walls. It also includes the corresponding RC wall stiffness equations. It is evident from the equations that the RC wall equations do not account for the reinforcement ratio, or the special composite behavior of SC walls.

For the reinforcement ratios (1.8-4.2%) used in the US-APWR project, this limitation does not have a significant influence. This is demonstrated in the table provided below, which includes the calculated stiffness values for the typical US-APWR SC wall with **[**

]

As shown, for condition “A”, the SC specific in-plane shear stiffness and axial stiffness are within **[** **]** of the corresponding RC values, and the SC specific flexural stiffness is **[** **]** of the corresponding RC value. The lower flexural stiffness is due to the fact that SC walls tend to crack early in flexure due to locked-in shrinkage strains and lower degree of composite action. For condition “B”, the SC specific in-plane shear and axial stiffness are within **[** **]** of the corresponding RC values, and the SC specific flexural stiffness is approximately **[** **]** larger than the corresponding RC values. The higher flexural stiffness is due to the higher reinforcement ratio (2%) in SC walls.

The most important comparisons in the table above are those related to the in-plane shear stiffness, because they dominate the lateral load (seismic) behavior of the CIS. As shown the in-plane shear stiffness calculated using SC specific equations were within **[** **]** of the corresponding RC values. This further verifies the adequacy of using either the SC specific or the RC wall stiffness equations published in ASCE 43-05 for SC-type walls specific to the US-APWR project (reinforcement ratios 1.8%-4.2%).

Based on this discussion, for Category 2 and 3 SC-type walls, the stiffness and damping values are based on those of RC walls published in ASCE 43-05, and summarized as follows:

The Category 2 SC-type walls are demonstrated in this TeR to remain effectively uncracked for loading condition “A”. They are assumed to be fully cracked for loading condition “B”. The Category 3 primary shield structure SC-type walls are demonstrated to remain uncracked for both loading conditions “A” and “B” in the TeR. For loading condition “B” (accident thermal), the primary shield structure remains uncracked due to significant restraint from the surrounding massive RC structure, and its large thickness.

The stiffness and damping values for category 4 and 5 RC structures are based on values published in ASCE 43-05, and summarized as follows.

The Category 4 RC slabs are demonstrated in this TeR to remain effectively uncracked for loading condition “A”. They are assumed to be cracked in flexure for loading condition “B”. The Category 5 massive RC structures are assumed to remain uncracked for both loading conditions “A” and “B” in this TeR due to their significant size, thermal inertia, and thickness.

The stiffness and damping values for Category 6 steel structures with non-structural concrete infill are based on the stiffness of the steel structure alone. The mass associated with the non-structural concrete infill is included directly in the models, but the concrete is not accorded any structural stiffness.

Thus, the stiffness and damping values for the different structure categories of the CIS are based on experimental results, understanding of structural behavior, good engineering judgment, and deliberate use of RC standards and codes endorsed by the USNRC. The development of these stiffness and damping values are presented in more technical detail in this TeR.

1.0 INTRODUCTION

1.1 Purpose

The purpose of this TeR is to define appropriate stiffness and damping values for use in structural analysis of the US-APWR CIS. Within the overall CIS design and validation methodology presented in TeR MUAP-11013 (Reference 2), this report presents the basis for the structural properties assigned to the Finite Element (FE) analysis models that support Task 1-A, “Dynamic SSI Analysis”; and Task 1-B, “Seismic Analysis for Structural Design," both of which are described in TeR MUAP-11013.

1.2 Objectives

The fundamental goal of the Task 1-A and 1-B analyses is to accurately characterize the seismic demands on the structural members of the CIS and the critical equipment they support, including the reactor and the Reactor Coolant System. As both Tasks 1-A and 1-B will employ LEFE models to achieve this goal, it is necessary to calculate effective stiffness values that reflect the extent of concrete cracking anticipated in the CIS during the seismic response. Once the cracked stiffness values are ascertained, appropriate damping values are assigned that reflect the energy dissipation capability of the cracked members.

As explained in MUAP-10006 (Reference 3), the FE models used for the SSI and subsequent structural analyses will be Three-Dimensional (3-D) LEFE models. They will not be lumped mass stick models due to the limitations of such models. Assessing the effects of concrete cracking on stiffness of the 3-D LEFE models is not straightforward because the CIS is made up of different structure categories that have varying response levels under applied loads and thermal conditions. For example, an overall percentage-type stiffness reduction would not be appropriate because of the varying responses of different structure categories under applied loads and thermal conditions. Similarly, the $1/10^{th}$ scale test of a related CIS structure presented in MUAP-11005 (Reference 4) cannot be used to estimate the stiffness for the 3-D LEFE models because: (1) it measures and provides only the overall (lumped) stiffness of the structure, not the stiffness of the individual members (walls etc.) of different categories. (2) the test structure had some deviations from the US-APWR CIS, which further limit the use of the overall structure stiffness. (3) the $1/10^{th}$ scale test does not include the combined effects of three spatial earthquake components, or the effects of thermal conditions on the overall stiffness. Therefore, the approach for defining stiffness values for the CIS must meet the following objectives:

1. Best-estimate stiffness values must be calculated for each of the structure categories in the CIS (as described in Section 2.0 below), based on their unique behavioral characteristics.

2. The stiffness values estimated for each category must account for the range of concrete stresses and resulting concrete cracking levels anticipated for the seismic loading conditions to which the structure may be exposed, including:
    - Seismic loading during normal operations
    - Seismic loading during Loss of Coolant Accident (LOCA) conditions.

    The variation in stiffness values produced by these two conditions necessitates two separate analyses, and the results of these analyses must be enveloped.

3. For structures in which the best-estimate stiffness values approach the uncracked or cracked values, a bounding analysis approach should be applied wherein the uncracked stiffness is used in the first analysis and the cracked stiffness is used in the second analysis. This ensures that inherent uncertainties in the loading inputs and analysis methods do not result in underestimated demands. The conservatism of this bounding approach must be verified by ensuring that the input motion dominant frequency does not fall within the range of fundamental frequencies produced by the uncracked and cracked stiffness estimates.

4. The stiffness and corresponding damping values estimated for each of the two analyses should be applied consistently to the models supporting Tasks 1-A and 1-B. Damping values assigned to the SSI analysis model (Task 1-A) must be appropriate for generation of ISRS, in accordance with United States Nuclear Regulatory Commission (USNRC) Regulatory Guide 1.61 (see Reference 5).

1.3 Approach and Report Overview

The following steps were taken to meet the objectives stated above for characterizing the CIS stiffness and damping, and will be described in detail in this TeR:

1. *Define Structure Categories*: Define the structure categories in the CIS in order to differentiate and group the walls and slabs based on their expected behavior. This step is discussed in Section 2.0.
2. *Define Loading Conditions*: In consideration of the design load combinations for the CIS, identify the basic loading conditions that must be considered to assess the potential range of concrete stresses and attendant cracking in each of the structure categories. This step is discussed in Section 3.0.
3. *Define Category-Specific Stiffness and Damping*: Define stiffness equations and damping values that are specific to each structure category. These are obtained from available codes and/or regulatory guidance for RC structures and are based upon experimentally verified values for SC structures. This step is discussed in Section 4.0.
4. *Evaluate Seismic + Normal Operating Condition*: Estimate the extent of cracking for seismic loading during normal operating conditions and assign appropriate stiffness and damping values for each category. This step is discussed in Section 5.0.
5. *Evaluate Seismic + Accident Condition:* Estimate the extent of cracking for seismic loading combined with accident conditions and assign appropriate stiffness and damping values for each structure category. This step is discussed in Section 6.0.
6. *Summarize Estimated Values:* Summarize the stiffness and damping values assessed for the two loading conditions and evaluate the feasibility of assigning overall damping ratios for each of the two corresponding analyses that would be appropriate for both ISRS generation and structural design. This step is discussed in Section 7.0.
7. *Application:* Apply the summarized stiffness and damping values to the analysis models. Calculate equivalent material properties for each wall and slab geometry that will produce the required stiffness terms and assign the properties to the elements of the Task 1-A and 1-B LEFE models. This step is discussed in Section 8.0.

2.0 STRUCTURE CATEGORIES[1]

As discussed above, the US-APWR CIS is comprised of a variety of structure types with significant differences in their construction and expected behavior. The structures in the CIS are classified into six categories to enable the use of appropriate analysis models and design methodologies for each of the structure categories. These six structure categories include three SC-type and three non-SC type categories, as explained in the following sub-sections. Figures 2-1 through 2-7 show several plan and elevation views of the US-APWR CIS that identify the six structure categories using a color-coded scheme. These figures have been developed from the drawings provided in References 5 and 6.

2.1 SC-type Structure Categories

The composite stiffness and strength of SC walls have been thoroughly established in experiments involving walls with an overall thickness less than or equal to **[ ]** Typical SC designs evaluated in these experiments consist of a single concrete core sandwiched between two steel faceplates, as shown in Figure 2-8. The steel faceplates are typically connected to the concrete core using headed stud anchors or embedded steel shapes, and the two steel faceplates are typically connected to each other using embedded steel shapes, tie bars, or web plates. The steel faceplate reinforcement ratios (ρ) in the experimental database vary between 1.5% and 5.0%, with ρ defined as follows:

Equation (2-1)
$$\rho = \frac{2 \cdot t_p}{T}$$

where t_p is the single faceplate thickness and T is the thickness of the overall section.

Most of the SC-type walls in the US-APWR CIS have material and geometric parameters that are within the range evaluated by the aforementioned experimental database. However, some of the walls have overall thicknesses and/or steel plate geometries that exceed this range. In these cases the fully composite stiffness cannot be assumed. Hence, the SC-type walls in the CIS are divided into the following three categories:

Category 1: *SC Walls with thickness less than or equal to 56 in.* These SC walls have material and geometric parameters that are within the range of the experimental database. This category includes the majority (approximately 80%) of the secondary shielding walls in the CIS. **[ ]**

Category 2: *SC Walls with thickness greater than* **[ ]** This category includes a relatively small portion of the CIS SC walls with thicknesses ranging from **[ ].**

Category 3: *Primary Shield Walls.* The primary shield walls below elevation **[ ]** range in thickness from **[ ]** They have a multi-cellular arrangement comprised of two steel faceplates, a mid-thickness steel plate, and numerous transverse web plates.

[1] The information in this section is also provided in TeR MUAP-11013 (Reference 2).It is repeated in this TeR for clarity.

2.2 Non-SC Structure Categories

The non-SC type walls in the CIS are classified into three additional structure categories:

Category 4: RC s*labs.* Standard RC floor slabs are used at various elevations throughout the CIS.

Category 5: *Massive RC.* This category includes the thick RC blocks at the base of the CIS that support the steam generators and reactor coolant pumps. These blocks are nominally **[ ]** deep and are anchored to the basemat of the R/B complex with steel reinforcement.

Category 6: *Steel structures with nonstructural concrete infill*. These structures consist of steel plates or steel shape grillages with nonstructural concrete provided for shielding purposes.

The US-APWR CIS also includes steel members that support the elevated RC slabs at elevations **[ ]**, as well as extensive secondary framing provided for support of operating platforms at various elevations. The columns that support the perimeter of the RC slabs are explicitly modeled in the SSI and detailed design models in order to provide the correct vertical load path and boundary conditions for the slabs, but the remainder of the secondary framing is included only as mass. In either case, the relative contribution of the steel framing stiffness and damping to the dynamic response of the primary structure is considered insignificant, such that these members are not included in the major structure categories identified for evaluation in this TeR.

Security-Related Information – Withheld Under 10 CFR 2.390

Figure 2-1 CIS Structure Categories, Elevations 3'-7" to 21'-0"

Figure 2-2 CIS Structure Categories, Elevations 21'-0" to 35'-11"

Security-Related Information – Withheld Under 10 CFR 2.390

Figure 2-3 CIS Structure Categories, Elevations 37'-9" to 62'-4"

Security-Related Information – Withheld Under 10 CFR 2.390

Figure 2-4 CIS Structure Categories, Elevations 62'-4" to 76'-5"

Figure 2-5 CIS Structure Categories, Elevations 76'-5" to 139'-6"

Security-Related Information – Withheld Under 10 CFR 2.390

Figure 2-6 CIS Structure Categories, Centerline Section Looking West

Security-Related Information – Withheld Under 10 CFR 2.390

Figure 2-7 CIS Structure Categories, Centerline Section Looking North

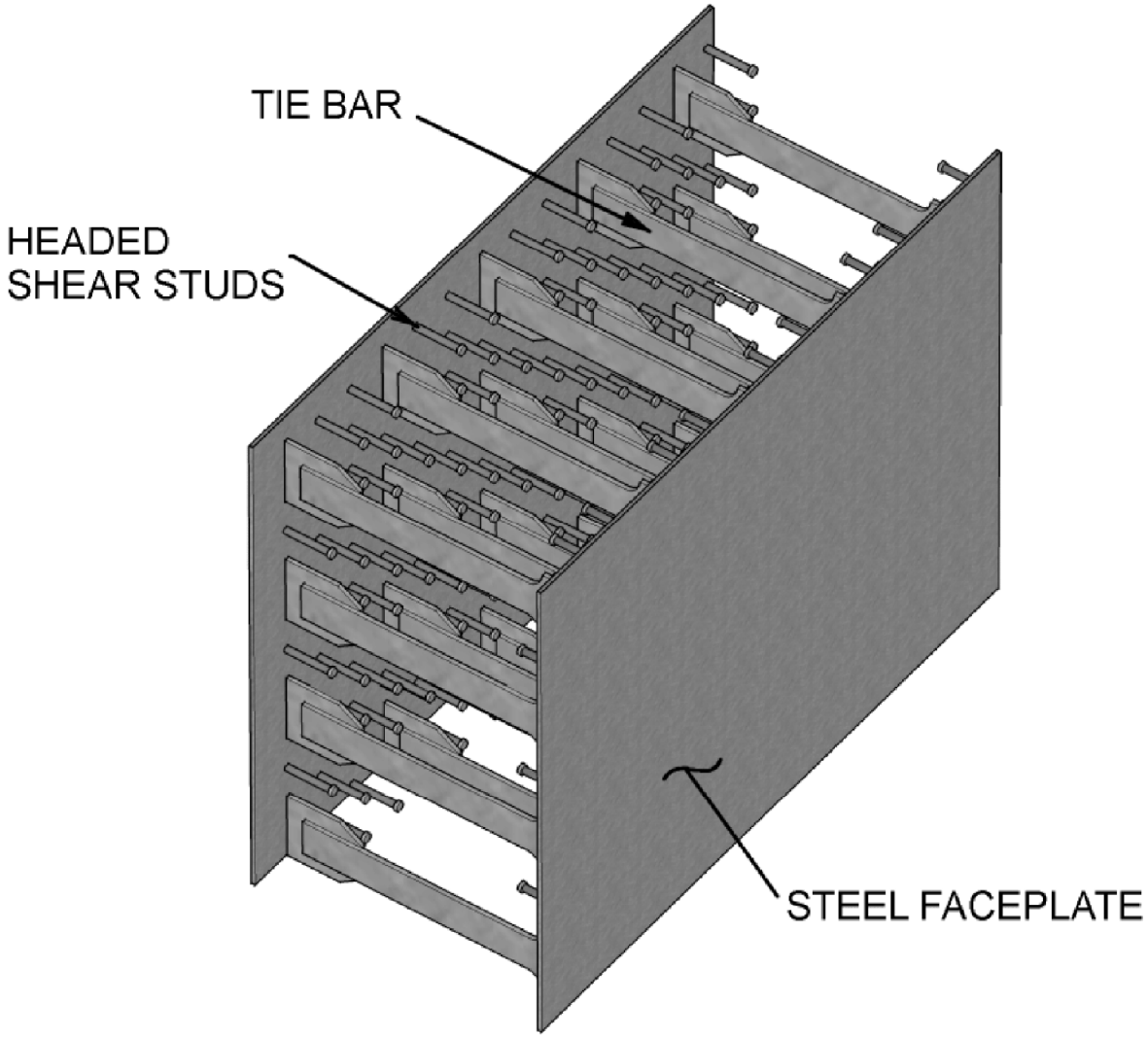

Figure 2-8 Typical SC Module Geometry

3.0 LOADING CONDITIONS FOR ASSESSMENT OF CRACKING

Assessment of load-induced concrete cracking for the CIS originates with identifying the specific load cases that will cause stresses that exceed the cracking stress of concrete and the combinations of these load cases that must be considered per regulatory guidance.

3.1 Design Load Combinations

The factored design load combinations for the CIS are governed by NRC Regulatory Guide 1.142 (Reference 6) which states that concrete structures within a containment structure may be designed in accordance with the strength design provisions of American Concrete Institute (ACI) 349-97 (Reference 7). Regulatory Guide 1.142 approves the load combinations given in Section 9.2.1 of ACI 349-97, which are the same as those provided in Appendix C of the ACI 349-06 (Reference 8) code specified for use on the US-APWR project. Several load factor modifications are required per the regulatory guide, which are included in the table of load combinations given in Table 3-1.

The site-independent seismic design of the US-APWR sets the Operating-Basis Earthquake (OBE) ground motion at one-third of the Safe-Shutdown Earthquake (SSE). This eliminates the requirement for performing explicit design analysis and load combinations containing OBE. As a result, the design load combinations that contain seismic loading are condensed to combinations 4 and 8 in Table 3-1. The evaluation of stiffness and damping for the CIS must address the extent of concrete cracking resulting from these two load combinations.

Besides seismic loading (E_{ss}), the most significant load cases in these two load combinations, in terms of their potential to crack the thick concrete members of the CIS, are the thermal loads, including operating thermal loads (T_o) and accident thermal loads (T_a). The results from analysis of the CIS prepared for basic design (see Reference 9) indicate that static dead (D), live (L), fluid (F), and accident pressure (P_a) loads result in minimal stress levels that will not cause significant concrete cracking in any of the CIS structures. As a result, loading combinations 4 and 8 from Table 3-1 may be reduced to the following basic loading conditions for assessment of concrete cracking in the CIS:

(**Equation 3-1)** Condition "A": $E_{ss} + T_o$

(**Equation 3-2)** Condition "B": $E_{ss} + T_a$

The following sections provide the details specific to the US-APWR CIS for each of the load cases in these two basic loading conditions.

3.2 CIS Seismic Loading

The CIS is a Seismic Category I structure to be evaluated for SSE seismic loading in accordance with Regulatory Guide 1.29 (Reference 10). Due to the irregularity of mass and stiffness in the CIS structure and the supported Reactor Coolant Loop (RCL), a dynamic analysis is used to determine the load path characteristics of the CIS. This analysis is performed using 3-D FE models developed for SSI analysis (Task 1-A) and structural design (Task 1-B).

A series of site-independent SSI analyses are performed for the R/B complex using eight generic soil profiles. These analyses are performed with the ACS SASSI program using a coarse-meshed 3-D FE model that includes the R/B mat, the R/B, the Prestressed Concrete

Containment Vessel (PCCV) and the CIS (see Reference 11). The dynamic properties of the CIS portion of the ACS SASSI model were derived from and validated against the detailed, refined mesh model developed in ANSYS for the CIS basic design (Reference 9).

The inertial seismic loading is obtained from the site-independent SSI analyses in the form of ISRS at the base of the CIS that are used as input to response spectrum analyses in ANSYS for structural design. ISRS are also obtained from the site-independent SSI analyses for design of equipment components and supports at various locations in the structure. The design ISRS represent the broadened and enveloped spectra generated for eight generic soil profiles, as discussed in Reference 11. The ACS SASSI analyses also provide enveloped time-history acceleration data at points throughout the CIS that are used to verify that the ANSYS response spectrum analyses sufficiently capture the accelerations resulting from the overall dynamic response of the soil-structure system.

Both the SSI and detailed ANSYS analyses consider the hydrodynamic response of the refueling water to seismic base motion. For purposes of assessing stiffness, the hydrodynamic response is computed for the operating condition, during which the refueling water is housed in the RWSP. The hydrodynamic response of the refueling water consists of the response of the impulsive mass acting rigidly with the walls of the RWSP, and the very low frequency convective or “sloshing” response of the convective mass. The manner in which these masses were computed and included in the analysis models is further discussed in Reference 9.

3.3 CIS Thermal Loading

The two basic loading conditions identified for evaluation of CIS stiffness and damping are differentiated by the associated thermal conditions. The design temperatures for the various compartments of the CIS during normal operating and accident thermal conditions are calculated in Reference 12 and summarized in the sections below.

3.3.1 Normal Operating Thermal Loads

The normal operating design temperatures in all of the CIS compartments except the reactor cavity are 105°F in the winter and 120°F in the summer. Since the ambient temperatures in these secondary compartments are equal in magnitude at any point in time, the walls and slabs that form the compartments experience steady state, uniform through-thickness temperatures. As a result, no significant concrete cracking is anticipated that would reduce the in-plane stiffness of the secondary compartment walls and slabs. However, thermal growth due to the net increase from construction temperatures (70°F) to operating temperatures may cause flexural cracking wherever the growth is restrained. A preliminary analysis of the CIS was performed to evaluate the extent of flexural cracking resulting from the 50°F temperature increase caused by the summer operating condition. The minimal stresses shown in the analysis results indicate that this condition will not cause significant flexural cracking in any of the walls and slabs of the secondary CIS compartments.

The normal operating temperature in the reactor cavity is 150°F. This results in a linear temperature gradient through the thickness of the primary shield walls of 30°F during summer operations and 45°F during winter operations. These shallow linear gradients through the thick primary shield walls will not cause significant concrete cracking. Appendix F provides a detailed explanation for this assessment in which it is demonstrated that linear thermal gradients result in minimal changes to mechanical stresses caused by structural loads.

Given the limited effects of the uniform temperatures applied to most of the CIS and the shallow linear gradients applied to the primary shield structure, the normal operating thermal load case is assessed to cause minimal concrete cracking in the CIS. As a result, the extent of concrete cracking for Condition ”A” will be taken as that induced by safe-shutdown seismic loading only. This is consistent with the objective to treat Condition ”A” as a rational upper-bound stiffness condition, to be considered in conjunction with the reduced stiffness associated with Condition ”B”.

3.3.2 Accident Thermal Condition

The accident thermal loading condition for the CIS occurs as a result of a postulated high-energy pipe rupture associated with a LOCA. Thermal hydraulic analyses are used to calculate the thermal transient conditions occurring in the compartments of the CIS following a high-energy pipe rupture in either the reactor cavity or one of the four SG compartments, as described in Reference 12. As a result of the refinements to the thermal hydraulic analyses, the input thermal loads have been revised from those considered in Revision 0 of this document as summarized in Appendix J.

The design accident thermal loading conditions for the CIS compartments are presented in the form of compartment air temperature vs. time plots that envelope the multiple postulated high energy line breaks in each compartment. These air temperatures are applied to the surface of the structure, and in some cases are reduced in consideration of surface condensation. The temperature envelopes for accident thermal transient conditions in the SG compartments and the reactor cavity are presented in Figures 3-1 and 3-2, respectively.

As shown the ambient temperature inside the compartment containing the ruptured pipe increases rapidly from operating temperature to between 450^{o}F and 550^{o}F , and then reduces with time. Because the various CIS compartments are open to the containment atmosphere, the ambient temperature in the containment atmosphere also increases rapidly from the operating temperature to 200°F, and then to 300°F within 10 seconds, as shown in Figure 3-3.

As discussed in Section 6.0, the structural surface design temperature time histories are input into heat transfer analyses to calculate the temperature gradients that form through the thickness of the walls and slabs of the CIS, and to determine the variation of these gradients with respect to time. In general, the steep parabolic gradients that develop shortly after the accident occurs induce high membrane tensile stresses that exceed the concrete cracking stress. In addition, the accident thermal condition causes a significant net temperature increase in the CIS walls and slabs, which results in significant thermal growth and flexural cracking where the growth is restrained. Further discussion of the specific effects of the accident thermal loading on each structure category is provided in Section 6.0.

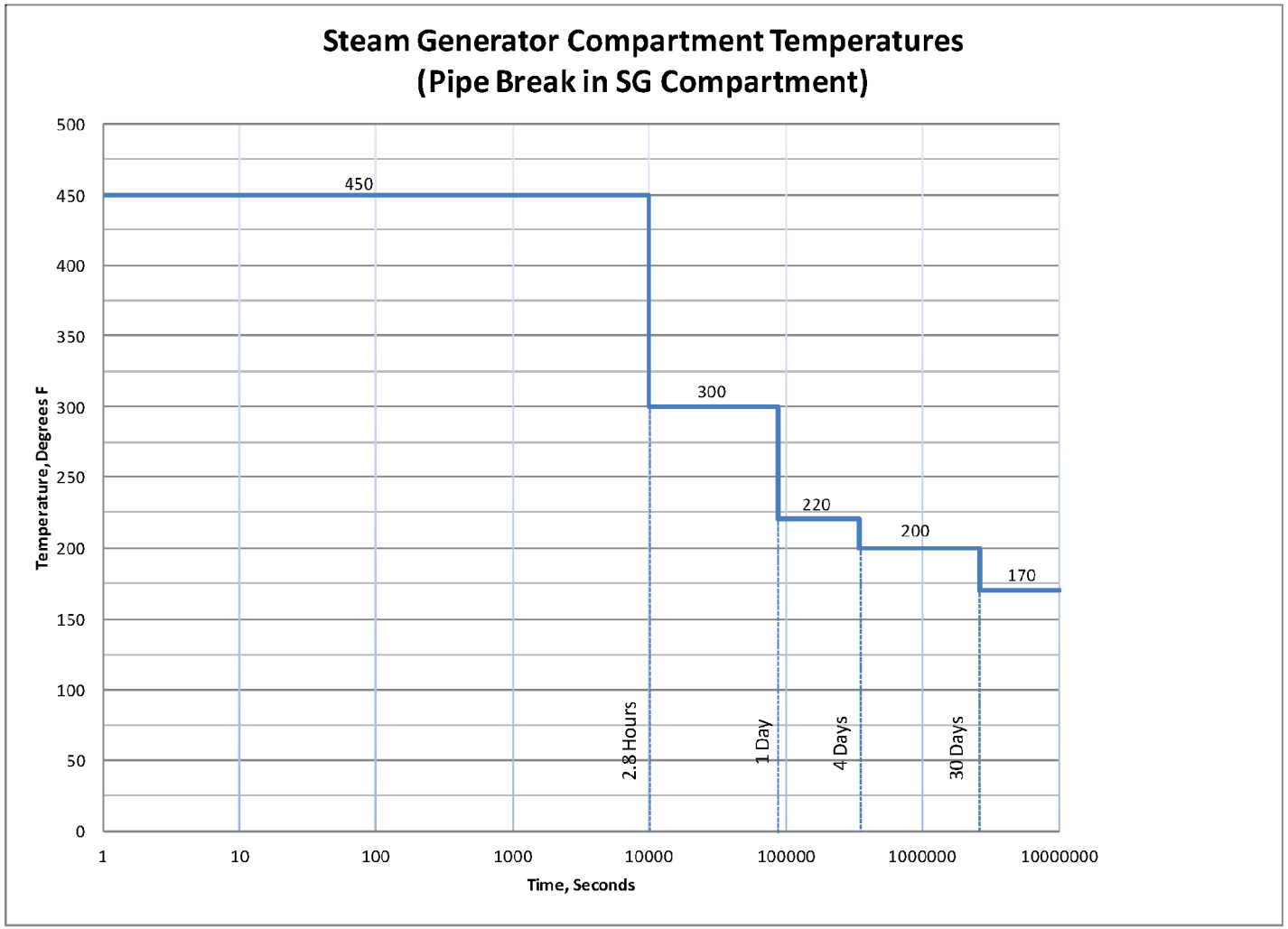

*Note: For structures with a certain heat capacity, such as walls, 450 deg F can be eased to 340 deg F (Reference 12)

Figure 3-1 Thermal Transient Envelope for Steam Generator Compartments

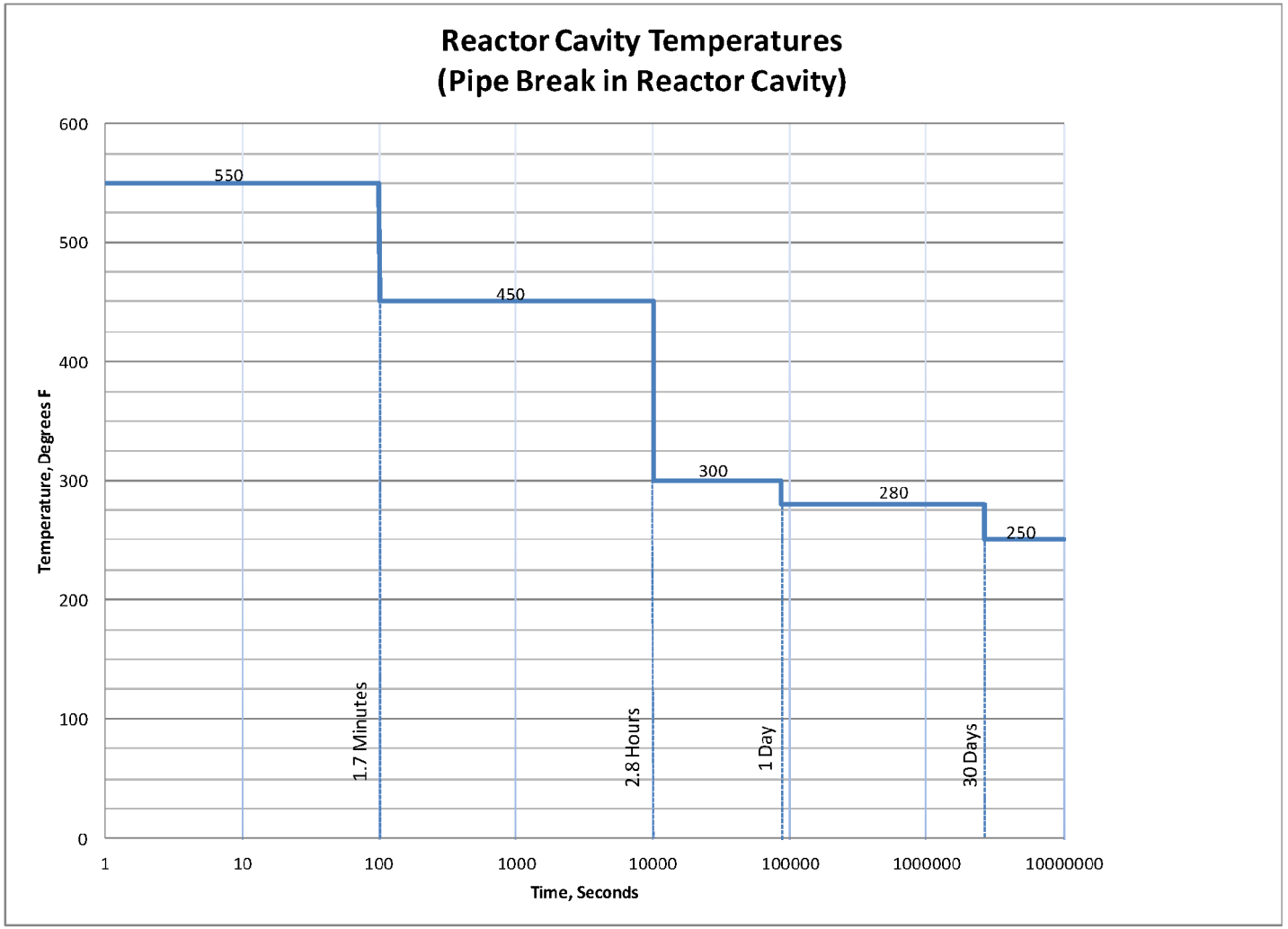

Figure 3-2 Thermal Transient Envelopes for Reactor Cavity

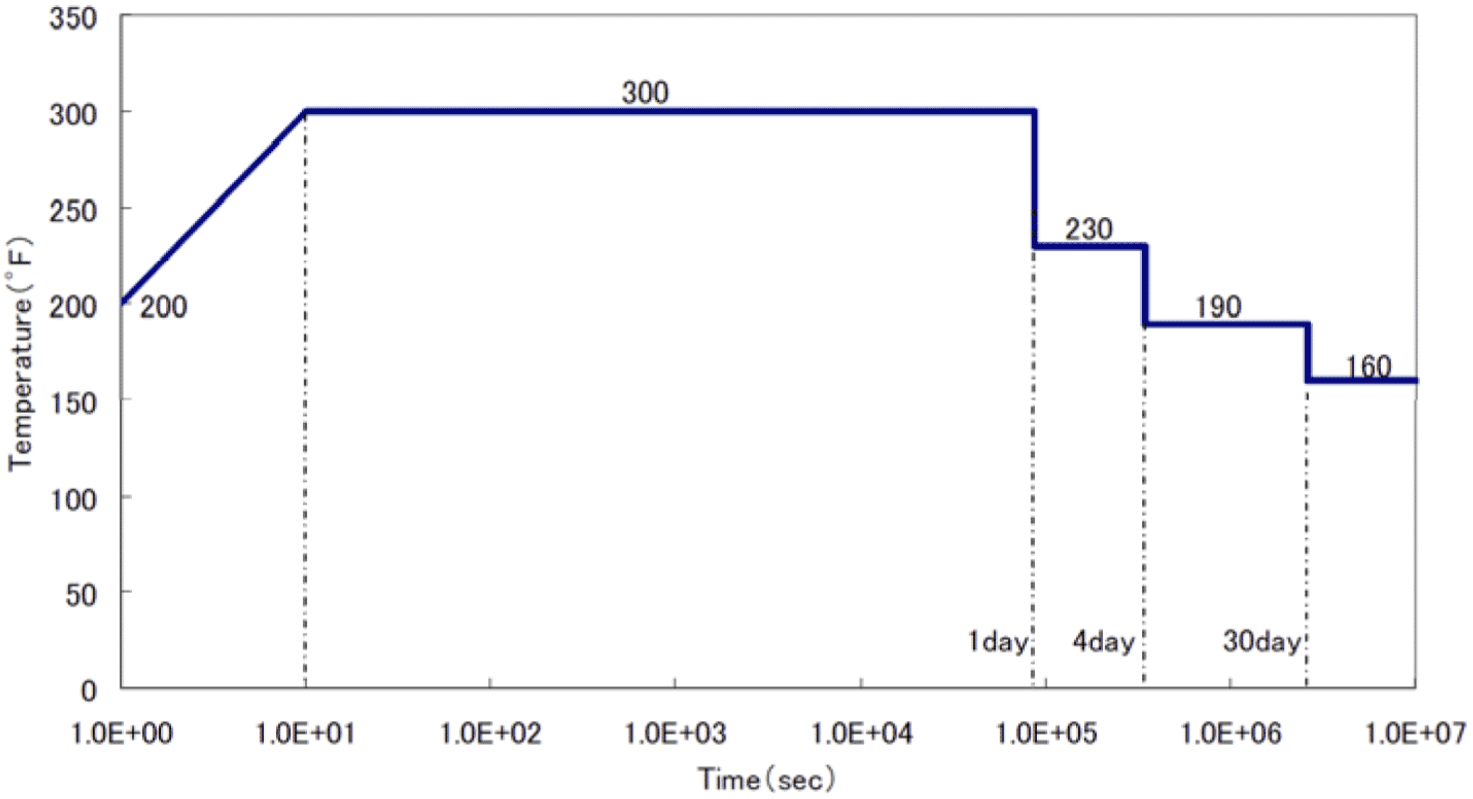

Figure 3-3 Thermal Transient Envelope for Containment Vessel Atmosphere

Security-Related Information – Withheld Under 10 CFR 2.390

Figure 3-4 Compartment Surface Temperatures for Accident Thermal Conditions following Pipe Break in Reactor Cavity

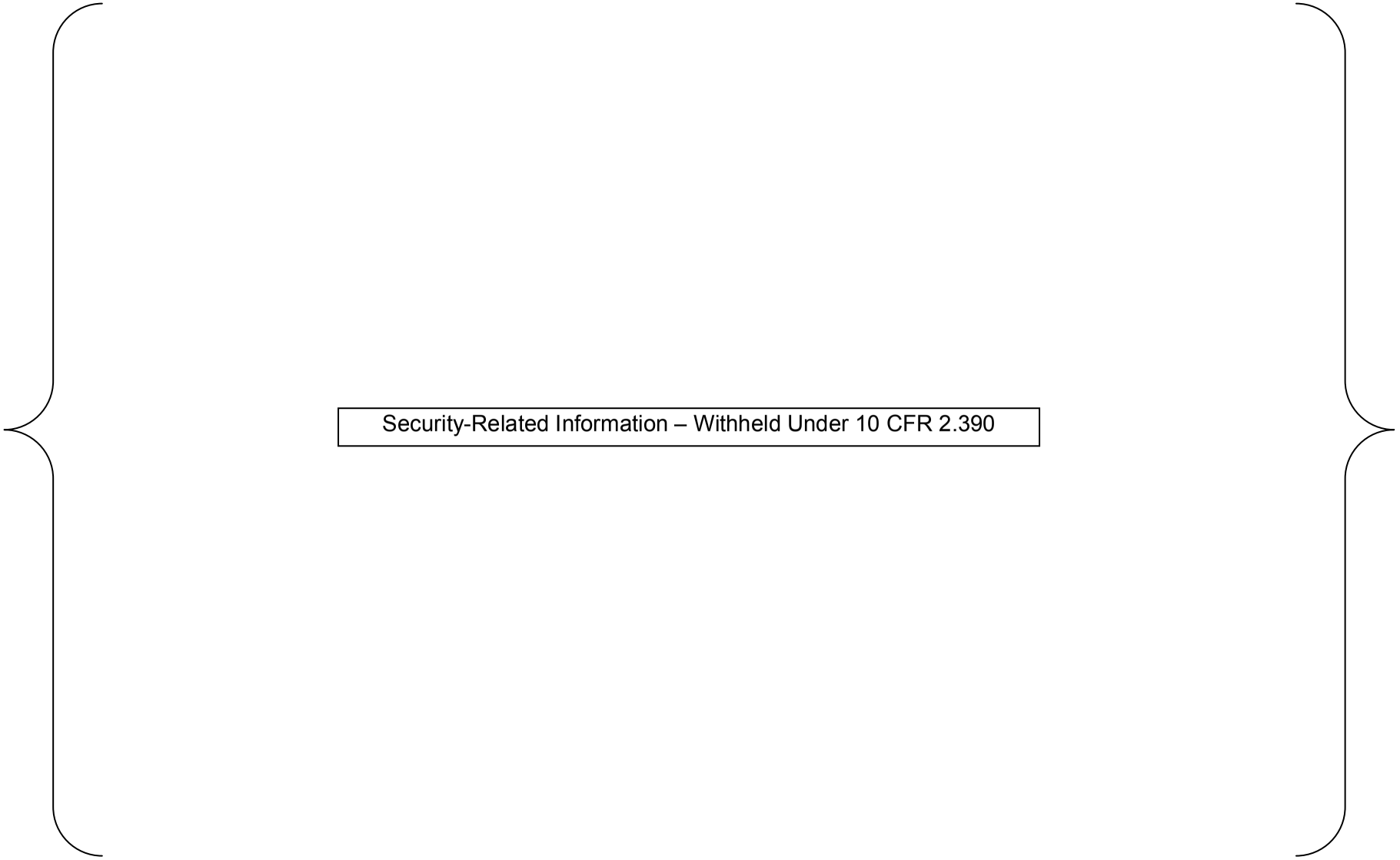

Figure 3-5 Compartment Surface Temperatures for Accident Thermal Conditions following Pipe Break in Steam generator Cavity

Table 3-1 Design Load Combinations for the US-APWR CIS

1. $U = 1.4D + 1.4F + 1.7L + 1.7H + 1.7R_o$
2. $U = 1.4D + 1.4F + 1.7L + 1.7H + 1.7E_o + 1.7R_o$
3. $U = 1.4D + 1.4F + 1.7L + 1.7H + 1.7W + 1.7R_o$
4. $U = D + F + L + H + T_o + R_o + E_{ss}$
5. $U = D + F + L + H + T_o + R_o + W_t$
6. $U = D + F + L + H + T_a + R_a + 1.4P_a$
7. $U = D + F + L + H + T_a + R_a + 1.15P_a + 1.0(Y_r + Y_j + Y_m) + 1.15E_o$
8. $U = D + F + L + H + T_a + R_a + 1.0P_a + 1.0(Y_r + Y_j + Y_m) + 1.0E_{ss}$
9. $U = 1.05D + 1.05F + 1.3L + 1.3H + 1.2T_o + 1.3R_o$
10. $U = 1.05D + 1.05F + 1.3L + 1.3H + 1.3E_o + 1.2T_o + 1.3R_o$
11. $U = 1.05D + 1.05F + 1.3L + 1.3H + 1.3W + 1.2T_o + 1.3R_o$

As given in ACI 349-06 Appendix C (Reference 8), with load factor modifications per Regulatory Guide 1.142 (Reference 6).)

4.0 CATEGORY-SPECIFIC STIFFNESS AND DAMPING

Before a detailed assessment can be made of the concrete cracking and associated stiffness reductions that result from the two loading conditions defined in Section 3.1, it is necessary to define generalized formulations for the stiffness and damping of each of the CIS structure categories. For the Category 1 SC walls, the stiffness and damping values are based on test results and verified models. As explained earlier, these stiffness and damping values are subsequently compared with those for equivalent RC structures to demonstrate their proximity and reasonableness. For the Category 2 and 3 SC walls, the stiffness and damping values of equivalent RC structures are used. For the Category 4 and 5 RC structures, the values used are those given in available codes and regulatory guidance for RC structures. The Category 6 structures are not modeled with any stiffness or damping for the nonstructural concrete; only the stiffness of the steel members is included. The following subsections provide further discussion of the basis for the individual stiffness and damping values considered for each structure category.

4.1 Category 1 SC Wall Stiffness and Damping

As discussed above, the majority of the secondary shielding walls in the US-APWR CIS are Category 1 SC walls. As a result, the in-plane shear stiffness of these walls comprises the primary lateral load resisting mechanism for the CIS and is therefore an essential component in the overall dynamic response of the structure. Modal analysis performed for the basic design (Reference 9) showed that the fundamental natural frequencies for lateral response of the CIS are directly related to the in-plane shear stiffness of these walls.

A reasonable characterization of SC wall in-plane shear stiffness must account for the significant contribution of the steel faceplates, both before and after cracking of the concrete core. The in-plane shear behavior of SC walls differs from that of RC walls because the continuous steel faceplates have a direct contribution to the in-plane shear stiffness of the composite wall. In RC walls, the reinforcing bars provide stiffness only in their axial directions and thus do not have a direct contribution to in-plane shear stiffness. It is important to note that the steel faceplates of SC walls are connected to the concrete infill and to each other with shear studs and tie bars. These connectors are typically designed to provide adequate composite action and strain compatibility between the steel plates and concrete infill as an engineering approximation. The experimental data discussed in the following sections demonstrate that composite action and strain compatibility (from an engineering perspective) can be achieved with reasonable shear stud size and spacing.

4.1.1 Uncracked In-Plane Shear Stiffness

Prior to cracking of the concrete core, the in-plane shear stiffness is estimated as the summation of the elastic shear stiffnesses of the concrete and steel, as follows:

In-plane shear tests performed by Ozaki, et al., (see Reference 13) demonstrate that Equation 4-1 provides an accurate estimate of uncracked stiffness for typical SC wall

geometries. As described in Appendix B, these tests used SC specimens with scaled geometries similar to those of the US-APWR CIS Category 1 walls, including reinforcement ratios (ρ) between 2.3% and 4.5%, and anchorage stud pitch to faceplate thickness ratios (*B/t*) of 30 to 31. (Reinforcement ratios for the CIS Category 1 walls vary from 1.8% to 4.2%, and a maximum *B/t* ratio of 16 is to be provided). Figure B.4A in Appendix B shows that the experimental in-plane shear stiffness values observed prior to cracking compared favorably to values calculated using Equation 4-1.

4.1.2 In-Plane Shear Cracking Threshold

As shown in Appendix A, uncracked in-plane shear stiffness is considered for the Category 1 SC walls when applied in-plane shear forces are less than or equal to the cracking shear force:

For RC applications, concrete cracking is typically assumed to occur when the maximum principal stress (which is equal to the shear stress for pure shear) exceeds the concrete tensile strength, equal to $4\sqrt{f'_c}$ (see Reference 14). As explained in Appendices A and B, the reduction of the cracking stress for SC sections to **[ ]** is considered the result of locked-in tensile stresses in the concrete due to restraint of curing shrinkage by the steel faceplates. Thus the cracking shear force (V_{ck}) for SC sections may also be defined as follows:

4.1.3 Cracked In-Plane Shear Stiffness

After cracking of the concrete core due to applied in-plane shear forces, the concrete offers very little in-plane shear stiffness in the principal direction perpendicular to the plane of cracking. However, the concrete does contribute resistance to the applied shears in the direction parallel to the plane of cracking, as explained in Appendix A. This is referred to as cracked orthotropic behavior of the SC wall concrete core. For the case of pure shear, the orthotropic stiffness of the concrete manifests as compression struts that form between the diagonally oriented shear cracks. The formation of concrete compression struts is possible in

SC construction because the steel faceplates provide confinement to the struts as well as resistance of the tension tie forces in the idealized response of the wall as a truss.

The post-cracking composite in-plane shear stiffness of SC walls is derived in Appendix A. The resulting bilinear shear-deformation relationship is shown in Figure 4-3. **[**

]

As presented in Appendix A, the post-cracking region of the bilinear shear-deformation curve terminates at the shear force that yields the steel faceplates according to the Von Mises yield criterion:

The theoretical composite response of SC walls to in-plane shear forces beyond the cracking threshold has been experimentally verified, both qualitatively and quantitatively. In the in-plane shear tests performed in Korea by Lee, et al., (see Reference 15), removal of the steel faceplates from the specimens after testing revealed a grid of through-thickness cracks oriented at 45 degrees to the applied in-plane shear force, demonstrating the expected composite response and the formation of compressive struts (see Figure 4-2). Furthermore, the ultimate shear strengths exhibited by the specimens were approximately equal to the yield

strength of the steel plates. This result is in accordance with Equation 4-7, given that these test specimens used similar reinforcement ratios to those specified for the US-APWR CIS. In addition, the values observed in the Ozaki tests for post-cracking shear stiffness and the yielding shear force were closely approximated by Equations 4-4 and 4-7, respectively, as shown in Appendix B, Figures B.4b and B.4d.

For the linear elastic analyses to be performed in support of Tasks 1-A and 1-B, secant stiffness values must be assigned to the SC walls in order to obtain a reasonable assessment of the dynamic response for the anticipated level of cracking. Secant stiffness values are calculated on the basis of the applied in-plane shear forces in the manner illustrated by Figure 4-3; i.e., the applied shear force is plotted on the bilinear shear-deformation curve and the secant stiffness is calculated for that point.

As shown in Figure 4-4, the calculated secant stiffness values decrease rapidly for applied shear forces just beyond the cracking threshold, and then approach a relatively constant value for a large range of in-plane shear forces that are well beyond the cracking threshold. Hence it is possible to define an empirical, best-fit formula that provides a reasonable approximation of the so-called “fully cracked” secant stiffness for the range of parameters included in the experimental investigations (that is, reinforcement ratios between 2% and 4.5% and shear stud b/t ratios less than or equal to 30) :

Further discussion of the basis for Equation 4-10 is provided in Appendix C. Figure 4-5 illustrates the calibration of Equation 4-10 to the fully cracked range of secant stiffness values for **[ ]**. Section 6.0 of this TeR discusses the applicability of this equation to the Condition “B” analyses.

4.1.4 Effective In-Plane Shear Stiffness

As discussed in Section 5.0, the secant in-plane shear stiffness will be estimated for each of the Category 1 SC walls for Condition “A” on the basis of the seismic in-plane shear forces calculated from preliminary response spectrum analysis of the CIS. These in-plane forces represent the maximum forces that are postulated to occur at any time throughout the duration of seismic shaking. Therefore the secant stiffness calculated using these forces represents the minimum stiffness exhibited, and is only appropriate for the last portion of the largest response cycle. The stiffness exhibited by the walls for all other response cycles will be higher than the calculated value.

According to research prepared for RC shear wall structures (see References 16 and 17), an effective stiffness value should be calculated for use in equivalent linear analyses that represents the aggregate of the stiffness values exhibited for all response cycles. The referenced research defined a calibrated relationship between effective linear stiffness and minimum secant stiffness by matching the maximum drift results obtained from a series of equivalent linear time-history analyses to those obtained with nonlinear time-history analyses. As discussed in Reference 17, for minimum secant stiffness values in the range of 0.25 to 1.0 times the initial stiffness, the calibrated relationship defined in the research can be approximated as follows:

Although the recommendations in the referenced research were specific to RC shear walls, they are also considered appropriate for use with SC shear walls. Reference 17 acknowledges that the hysteresis loops for in-plane shear response of SC walls may be slightly less pinched than for RC walls. However, this difference in behavior is deemed to have very little effect on the effective stiffness calibration presented in the research. It is only considered pertinent to the calculation of hysteretic damping.

4.1.5 Out-of-Plane Flexural Stiffness

As explained in Appendix E, experiments on SC walls subjected to out-of-plane flexure indicate that the uncracked composite flexural stiffness is never exhibited. Instead, the cracked composite stiffness is observed immediately upon application of loads that induce flexural stresses. There are several reasons given for this behavior. First, the concrete core of SC sections develops significant locked-in shrinkage stresses during casting. These stresses reduce the applied stress required to crack the concrete core. Also, the bond of the steel to the concrete in SC sections is not continuous as it is with deformed reinforcement in RC sections. Instead, the SC bond is intermittent, with connections only at the individual anchorage stud and tie bar locations. Since the anchorage studs have a certain degree of flexibility, a certain level of section rotation or slip is required to mobilize the steel plate reinforcement. In the

presence of locked-in shrinkage stresses, this rotation is sufficient to crack the concrete core prior to engagement of the reinforcement. Thus the uncracked composite stiffness of the SC section is never manifested.

As shown in Appendix E, the cracked composite flexural stiffness of SC walls may be approximated as the cracked-transformed flexural stiffness of the section. An empirical formula for the cracked-transformed stiffness is defined in Appendix E that distinguishes the steel and concrete stiffness contributions, as follows:

4.1.6 Axial Stiffness

Although the axial stiffness of the Category 1 SC walls is not considered to be as critical to the dynamic response of the CIS as the in-plane shear stiffness or out-of-plane flexural stiffness, the effects of concrete cracking on axial stiffness must still be considered. For the equivalent linear elastic analyses to be used for dynamic analysis of the CIS, the cracked axial stiffness assigned to the analysis models must try to capture both the reduced stiffness of the walls in tension and the gross stiffness of the walls in compression. Since this behavior cannot be modeled explicitly, it may be argued that an equivalent axial stiffness should be assigned that is equal to the average of the cracked and uncracked stiffness values:

However, this approach is somewhat questionable, since (a) the portion of the walls closer to the base of the structure will have dead load compressions that may not be overcome by seismic uplift forces, and (b) the axial force resultants in the walls due to overturning will not be of uniform magnitude across the plan of the structure.

Given these uncertainties, the approach taken for modeling the axial stiffness of the Category 1 SC walls utilizes the elastic modulus (E) and cross sectional area (A) generated by matching the effective in-plane stiffness (GA) and out-of-plane flexural stiffness (EI) defined for each analysis condition. As will be further discussed in Section 8.0, this approach results in rational values of axial stiffness for both the uncracked analysis (Condition “A”) and the cracked analysis (Condition “B”).

4.1.7 Damping

As summarized in MUAP-10002 (see Reference 18), the energy dissipation capability of SC walls was evaluated in the 1/10th scale test of a CIS performed by Akiyama, et al., (see also Reference 19). An equivalent viscous damping factor for cracked SC walls was calculated from the observed hysteretic curves by equating the energy dissipated in the actual structure (i.e., the area enclosed by the hysteretic loop) to the energy dissipated in an equivalent viscous system. The associated equation given in Reference 19 is as follows:

The energy dissipation characteristics of uncracked SC walls are considered to be similar to those of uncracked RC walls, for which a 4% damping ratio is given in Reference 5.

4.1.8 Effect of Stainless Cladding

Several of the Category 1 SC walls in the US-APWR CIS utilize stainless steel cladding for corrosion protection of the structural steel faceplates. In all cases, the stainless cladding is provided only on the interior faceplate that is exposed to water during plant operations. The Category 1 walls utilizing stainless steel cladding on their interior faceplates include the RWSP walls **[ ]** and the Refueling Cavity walls **[ ]**. The cladding consists of **[ ]**-thick **[ ]** material that is bonded to the **[ ]** faceplate using the hot roll bonding process, which creates a metallurgical bond between the layers via heating and deformation during rolling. Importantly, welding between adjacent modules with interior faceplate cladding is accomplished by first performing full-penetration welds between the carbon steel faceplates using carbon steel electrodes, and then providing separate seal welds in the cladding material using stainless welding electrodes and filler metals.

The stainless steel cladding on the SC walls is considered nonstructural for design purposes; its strength is not considered in calculating structural resistance to loads. However, from an analysis perspective the effect of stainless cladding on the Category 1 stiffness terms defined above must be evaluated. In general, it is reasonable to neglect any contribution of the cladding to either in-plane shear or out-of-plane flexural stiffness for two reasons:

1) The bond between the structural faceplate and the cladding material has uncertain reliability in terms of its ability to maintain strain compatibility between the two layers.

2) The nominal yield stress of the **[ ]** material is 25 ksi, or 50% of the nominal yield stress of the A572 faceplate material. As such, the thin stainless cladding layer will yield well in advance of the structural faceplate if the bond between the plates is maintained. Although the nominal elastic

modulus of **[** **]** the secant modulus exhibited by the **[** **]** plate material during design basis events will be substantially lower given its low yield stress. Thus the net effect of the stainless layer on overall SC wall stiffness during design basis seismic and accident thermal events will be minimal.

Going beyond these two considerations, calculations have also been prepared to evaluate the effect of stainless cladding on the in-plane shear and out-of-plane flexural stiffness terms for the RWSP and Refueling Cavity walls in question. This evaluation is provided in Appendix G, and the results are summarized below in Table 4-1. The calculations assume **[** **]**, such that the increases in stiffness due to cladding given in Table 4-1 are conservative.

Table 4-1 indicates that the in-plane shear stiffness increase associated with perfectly composite, elastic response of the cladding is between 2% and 6%. It is noted that in-plane stiffness is the more critical stiffness term for the dynamic response of a shear wall structure such as the CIS. The less influential out-of-plane flexural stiffness term increases between **[** **]**, depending on whether the cladding is on the tension or compression faceplate. The average increase in flexural stiffness to be considered under cyclic loading is therefore less than **[** **]**. Taken together, these small stiffness increases and the aforementioned general considerations regarding bond reliability and low stainless steel yield strength support the approach of ignoring the stainless cladding when calculating the Category 1 stiffness terms for the Task 1-A and 1-B analysis models.

4.2 Stiffness and Damping of Category 2 and 3 Walls

As discussed above in Section 2.1, the experimental database that confirms the composite stiffness characteristics of SC walls before and after cracking is limited to sections with overall thickness less than **[** **]** Some experimentation has been performed on the behavior of the primary shield structure (see Reference 20), but further study is required to ascertain that the composite behavior observed for this structure is fully consistent with that derived and experimentally verified for the Category 1 SC walls. Therefore the additional flexural and in-plane shear stiffness contributions from the steel plates will not be considered for the Category 2 and 3 walls. Instead, the stiffness and damping values for RC will be used. The sources referenced for these values are discussed below.

4.3 Stiffness and Damping of Category 4 and 5 Reinforced Concrete Structures

Stiffness and damping values for RC structures are provided in the currently available nuclear standards. Specifically, Table 3-1 of ASCE 43-05 (Reference 1) provides out-of-plane flexure, in-plane shear, and axial stiffness values for RC walls and slabs. These values are restated in Table 4-2 of this TeR. It is noted that the code specifies the values to be used on the basis of anticipated cracking. For out-of-plane flexural stiffness, cracked values are specified if the bending stress in the slabs or walls exceed the cracking stress. Cracked in-plane shear stiffness values are specified when in-plane shear forces exceed the nominal concrete shear capacity.

Regulatory Guide 1.61 (Reference 5) provides damping values for RC structures that are intended for use in OBE analyses and Safe SSE analyses. The damping levels specified (4% for OBE and 7% for SSE) are based on the expectation of limited cracking during response to the OBE accelerations, and extensive cracking associated with responses close to code stress limits under SSE loading.

In keeping with the approach identified in these standards, stiffness and damping values will be assigned to the structures of the CIS for each of the two loading conditions considered on the basis of anticipated cracking. The assessment of cracking for each condition is described in Sections 5.0 and 6.0.

4.4 Category 6 Modeling

As stated in Section 2.2, the Category 6 structures in the CIS consist of grillages of steel plates or shapes (e.g., wide-flange sections) that are filled with concrete for shielding purposes. The concrete in these structures is nonstructural, as it is not detailed to act compositely with the steel. Hence the CIS analysis models for Tasks 1-A and 1-B will include the stiffness of the steel members only. The concrete infill will be considered only as lumped mass on the steel structures.

Figure 4-1 Calculated vs. Experimental Cracking Shear Force

Figure 4-2 Diagonal Cracking Pattern in SC Panel Subjected to In-Plane Shear

As shown in Reference 15. The steel faceplate has been removed to observe the concrete core.

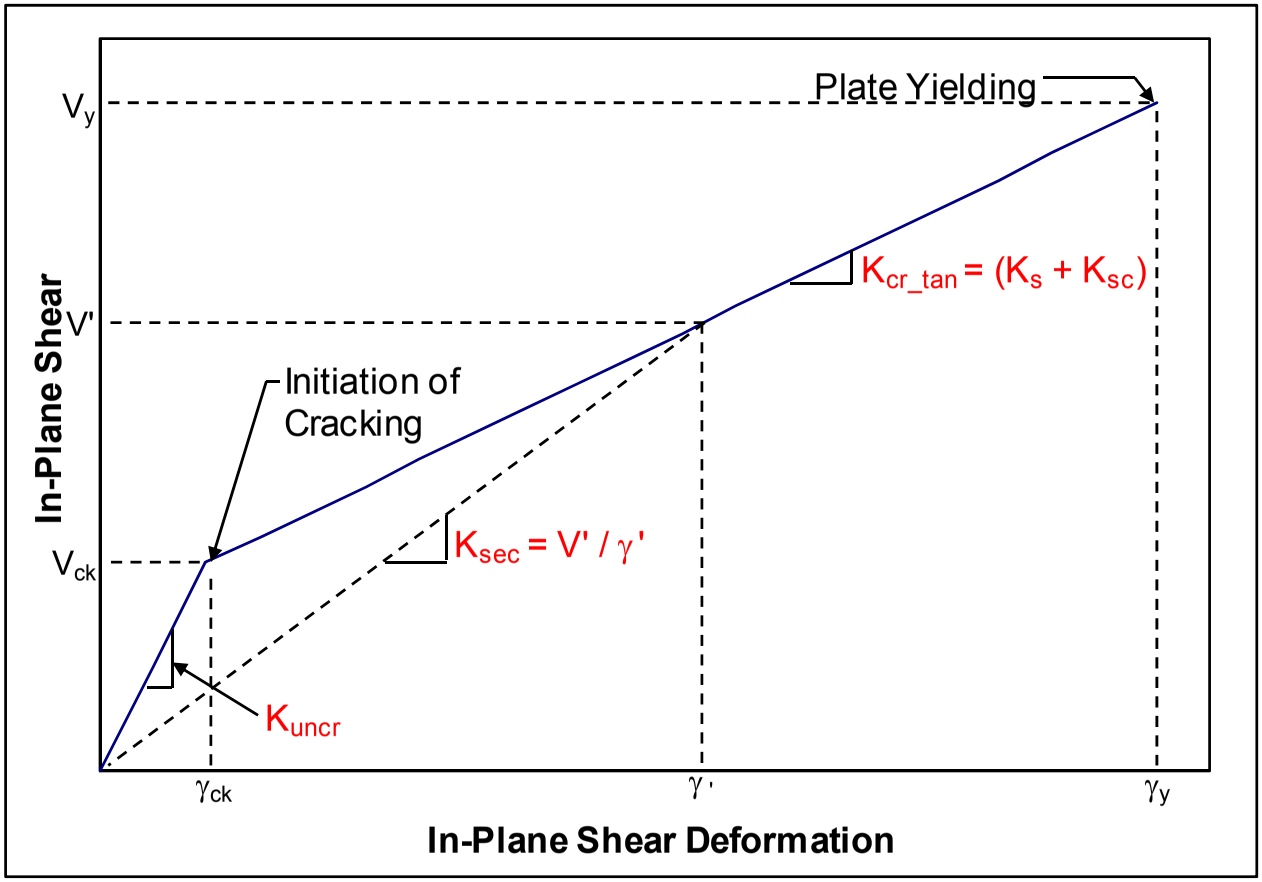

Figure 4-3 Bilinear Shear-Deformation Relationship for SC Walls

Figure 4-4 Secant Stiffness vs. In-Plane Shear Force for Category 1 SC Walls

The plot shows the range of normalized reinforcement ratios used in the US-APWR CIS.

Figure 4-5 Comparison of Equation 4-10 vs. Fully Cracked Secant Stiffness

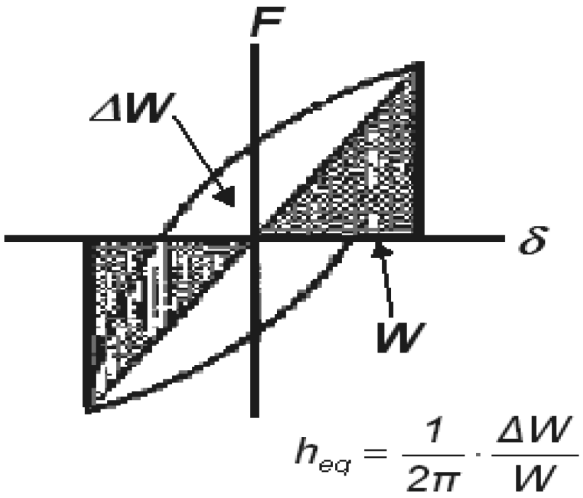

Figure 4-6 Equivalent Viscous Damping from Hysteretic Loop

(As given in Reference 19).

Table 4-1 Comparison of Category 1 Structure Stiffness Values Without/With Stainless Cladding

See Appendix G for the supporting calculations.

Table 4-2 Effective Stiffness Values for RC Walls and Slabs

As given in ASCE 43-05 (Reference 1).

5.0 EVALUATION OF STIFFNESS AND DAMPING FOR LOADING CONDITION "A"

As discussed in Section 3.0, the normal operating temperatures are not expected to cause significant cracking in any of the CIS structure categories. Thus the extent of cracking for Condition "A" may be reasonably estimated by evaluating stresses resulting from SSE loading only. As a result of refinements to the SSI seismic analysis, the input seismic loads have been revised from those considered in Revision 0 of this report as summarized in Appendix J.

To facilitate this evaluation, response spectrum analysis was performed using the detailed ANSYS model prepared for basic design of the CIS (Reference 9). For this evaluation, the analysis model used uncracked (full) stiffness values. The inputs to the analysis were three translational acceleration response spectra generated at the base of the CIS in the SSI analysis of the R/B complex described in Reference 11. In accordance with Regulatory Guide 1.92 (see Reference 21), the Lindley-Yow method was used to separate the rigid and periodic responses of the CIS for each direction of motion, and the periodic responses were combined using the Complete Quadratic Combination method. The rigid response was then calculated using the static zero-period acceleration method, and the periodic and rigid responses were combined by Square Root of the Squares (SRSS); i.e., Combination Method "B" was used. The hydrodynamic response of the refueling water in the RWSP was also included in each of the directional response components, as described in Reference 9. Finally, the three directional response components were combined by SRSS and added to the absolute value of the accidental torsion load case to obtain a total seismic load case representing the maximum earthquake-induced response of the CIS.

The paragraphs below present the evaluation of cracking and associated stiffness reductions that were performed for each of the structure categories using the initial seismic analysis performed as described in Appendix J. The evaluations are presented in the given order to simplify explanation of the approaches taken. The results of these evaluations are summarized in Section 7.0 and in the list of stiffness and damping values given in Table 7-1.

5.1 Category 1 In-Plane Shear Stiffness Evaluation

The following procedure was applied to determine appropriate values for the in-plane shear stiffness of the Category 1 SC walls under Condition "A":

1. *Group the SC wall elements in the model into collections of elements that form individual walls in the structure*. This procedure was performed in ANSYS using element "components," which can contain any selected set of elements and can be given an appropriate name. The SC wall components were generally selected such that all elements in the component may be considered to act together as a wall that transfers in-plane shear from one floor to another in a given direction. Thus the components include elements with common cross-sectional properties and typically have boundary conditions comprised of a slab or mat at the bottom edge, a slab at the top edge, and transverse walls at either end. The ANSYS plot in Figure 5-1 shows one example of the 96 components defined in this fashion.

2. *Calculate the uncracked in-plane shear stiffness for each wall component geometry*, using Equation 4-1.

3. *Extract the seismic in-plane shear forces on each wall component and calculate the secant stiffness for the wall*. In order to automate this procedure, a routine was written in ANSYS that assumed the overall shear applied at the top of the wall is

distributed to the elements of the wall on a per-foot basis. This assumption was deemed reasonable for the manner in which the elements were grouped in step 1, and was subsequently verified by hand calculations that considered the wall as a whole. The ANSYS routine extracted the seismic in-plane shear force on each element and calculated the element secant stiffness using the bilinear shear deformation curve as described in Section 4.1.3. The element secant stiffnesses were then averaged to obtain the secant stiffness of the wall.

4. *Compute the ratio of secant stiffness to uncracked stiffness* using the results of steps 2 and 3.

5. *Compute the ratio of effective stiffness to uncracked stiffness* using Equation 4-12, recalling that the initial stiffness is considered the uncracked stiffness for Condition “A”.

The results of this procedure are shown in Table J-1. The calculated effective stiffness values are shown to be close or equal to the uncracked stiffness for a majority of the SC walls, which indicates that the seismic in-plane shear demands are relatively low for the thick wall geometries provided in the CIS. In accordance with the third objective stated in Section 1.2, the tabulated results support the use of the composite uncracked in-plane shear stiffness for all of the Category 1 walls under Condition “A”, recognizing that the cracked in-plane shear stiffness is to be used for Condition “B” (as will be discussed further in Section 6.0). This approach will capture the reduced stiffness values calculated for some of the walls in the present evaluation.

As mentioned in Section 4.1, the out-of-plane flexural stiffness for the Category 1 SC walls is taken as that of the cracked-transformed section for all loading conditions. Since the in-plane shear stiffness of these walls has a more significant impact on the CIS dynamic response, the uncracked damping ratio of 4% discussed in Section 4.1.7 is considered appropriate for the Category 1 walls under Condition “A”.

5.2 Category 4 Out-of-Plane Flexural Stiffness Evaluation

The primary dynamic response of interest for the Category 4 floor slabs is their out-of-plane (vertical) response. Thus the results of the initial seismic analysis were also used to evaluate the extent of out-of-plane flexural cracking in each of the major floor slabs. The following procedure was applied to determine appropriate stiffness values for the Condition “A” analyses, in accordance with ASCE 43-05 (Reference 1):

1. *Group the RC slab elements in the ANSYS model into components*. Five major RC slabs were identified in the CIS structure, including slabs at top-of-concrete elevations 25 ft.-3 in., 37 ft.- 9 in., 50 ft-2 in., 76 ft.-5 in., and 139 ft.-6 in. The locations of these slabs are shown in Figures 2-1 through 2-7.

2. *Combine the total seismic case with dead load to create two load cases*: *Dead Load + Seismic Load, and Dead Load - Seismic Load*. These two cases must be considered to include the flexural stresses due to the structure dead load and because the signs of the seismic stress resultants are lost in the SRSS procedures discussed above.

3. *For each element in a given slab, extract the out-of-plane moments MX, MY, and MXY for each of the two loading conditions.*

4. *Calculate the maximum principal moments in each element, for each loading condition.* The following formulas are used:

(Equation 5-1) $$M_1, M_2 = \frac{MX + MY}{2} \pm \sqrt{\left(\frac{MX - MY}{2}\right)^2 + MXY^2}$$

(Equation 5-2) $$M_{max} = max\left(|M_1|, |M_2|\right)$$

5. *Calculate the cracking moment for each slab geometry,* using the formulas provided in ACI 349-06 Section 9.5.2.3 (Reference 8):

(Equation 5-3) $$M_{cr} = \frac{f_r I_g}{y_t}$$

(Equation 5-4) $$f_r = 7.5 \cdot \sqrt{f'_c}$$

where f_r is the modulus of rupture of concrete, I_g is the moment of inertia of the gross section per unit width, and y_t is half the thickness of the gross section.

6. *Compare the maximum principal moments in each element (from either load case) to the cracking moment, and calculate the percentage of elements that are cracked.*

The results of this procedure are shown in Table J-2. The computed maximum principal moments are shown to be less than the cracking moment for most of the elements in each of the five major slabs. The slab with the most elements cracked in flexure is the operating floor at Elevation 76'-5", in which **[ ]** of the elements are cracked. The ANSYS contour plot shown in Figure J-1 indicates that flexural cracking in this slab is limited to the region immediately adjacent to the secondary shield walls to which the slab is rigidly connected. Since most of the elements in each of the major slabs are uncracked, a bounding approach similar to that described for in-plane shear stiffness of the Category 1 walls is to be used for the RC slabs: the uncracked out-of-plane flexural stiffness is to be used for Condition “A”, recognizing that the cracked stiffness is to be used for Condition “B”. This will ensure that any modification of dynamic response due to flexural cracking is sufficiently covered in the enveloped results.

The Category 4 slabs do not carry significant in-plane shear forces under seismic loading. Thus the uncracked in-plane shear stiffness is assigned to the slabs for Condition “A”. Given that both the flexural and in-plane shear stiffness of the slabs are considered uncracked for this condition, a 4% damping ratio is assigned in accordance with the intent of Regulatory Guide 1.61 (Reference 5).

5.3 Evaluation of Concrete Stresses in Categories 2, 3, and 5

5.3.1 Category 2 Walls

As discussed in Section 4.2, the Category 2 walls are treated as RC structures in terms of their stiffness and damping characteristics. In accordance with ASCE 43-05 (Reference 1), the in-plane shear stiffness of these walls was evaluated for Condition "A" by determining the extent to which the applied seismic in-plane shear forces exceed the concrete in-plane shear strength. The concrete component of in-plane shear strength is calculated in accordance with ACI 349-06 Equation 21-7 (Reference 8) as follows:

(Equation 5-5) $$V_c = A_{cv}(2\sqrt{f'_c})$$

where A_{cv} is the cross-sectional area of the wall in the direction of the applied shear force and the concrete in-plane shear strength coefficient α_c is taken equal to 2.0.

Figure J-2 presents an ANSYS contour plot of the seismic in-plane shear forces (N_{XY}) applied to the Category 2 walls that were modeled with shell elements, which includes the 67 in. -thick walls in the refueling canal area (this comprises a majority of the Category 2 walls). As shown in the plot, the in-plane shear forces in excess of the concrete shear strength are limited to a small portion of the walls. Therefore the uncracked in-plane shear stiffness is warranted for use with Condition "A", given that the cracked stiffness is to be used for Condition "B". It is noted that the stiffness considered will be that of the concrete section only, as is customary for RC sections.

To evaluate the out-of-plane flexural stiffness of these walls, a procedure similar to that used for the RC slabs was applied. Figure J-3 shows that the seismically induced maximum principal moments for the elements of the Category 2 walls were in all cases less than the cracking moment. Thus the uncracked out-of-plane flexural stiffness given for RC sections is to be used for Condition "A".

Given that these walls are considered uncracked for both in-plane shear and flexural stiffness, they are assigned a damping ratio of 4% for Condition "A", in accordance with the intent of Regulatory Guide 1.61 (Reference 5).

5.3.2 Categories 3 and 5

The Category 3 and 5 structures in the CIS are also treated as RC when evaluating the effects of cracking on their stiffness and damping properties. The Category 3 primary shield walls are not anticipated to experience seismically induced in-plane shears or out-of-plane moments beyond the cracking threshold, given their large cross-sectional thickness, their rigid cylindrical arrangement, and the fact that they are confined by the Category 5 massive RC over much of their height (see Figures 2-6 and 2-7). Likewise, the Category 5 sections themselves are not expected to experience seismically-induced cracking in light of their rigid geometries.

Both of these structure categories were modeled in ANSYS with 3-D solid elements. Thus it is necessary to evaluate the stated assumption of limited stresses under seismic loading by comparing maximum principal stresses to the tensile strength of concrete. Figures J-4 and J-5 present ANSYS contour plots for the Category 3 and Category 5 structures, respectively, of maximum principal stress due to a load case consisting of dead load plus total seismic load. This case is considered because the signs of component stresses in the total seismic load

case are all positive, such that the addition of the seismic load case to dead load maximizes tensile principal stresses in the output, while the dead load minus seismic load case results in more compressive principal stresses. As shown in the figures, principal stresses in excess of the tensile strength of concrete (taken as $4\sqrt{f'_c}$) are limited to small portions of both the Category 3 and Category 5 elements in the model. Therefore these structures are assigned uncracked RC stiffness and damping values for Condition “A”.

Figure 5-1 CIS ANSYS Model Showing Wall Component Selection

6.0 EVALUATION OF STIFFNESS AND DAMPING FOR LOADING CONDITION "B"

The evaluation of seismically induced concrete stresses discussed in Section 5.0 rendered the assessment that all of the structure categories in the CIS are largely uncracked for Condition "A". As discussed in Section 3.0, the addition of accident thermal loading is anticipated to result in significant concrete cracking of the various walls and slabs of the CIS. As a result of refinements to the thermal hydraulic analyses, the input thermal loads have been revised from those considered in Revision 0 of this Report as summarized in Appendix J.

6.1 Heat Transfer Analysis

When the accident thermal temperatures shown in Figure 3-1 occur in the compartments of the CIS, nonlinear temperature gradients will form through the thickness of the walls. In order to determine the magnitude and distribution of these temperature gradients with respect to time, heat transfer analyses were performed in support of the CIS basic design (Reference 9). These analyses utilized a finite difference approach wherein one-dimensional conduction was assumed through the thickness of the wall; i.e., the in-plane extents of the wall were considered infinite and uniform surface temperatures were assumed. The analyses also assumed that the steel faceplates on the walls directly conduct the ambient compartment temperatures to the faces of the concrete core, and that the concrete material properties are constant and isotropic.

Figure 6-1(a) shows the heat transfer analysis results for the **[ ]** Category 1 SC walls that are used extensively in the CIS and typically as the exterior walls of the SG compartments. The plot illustrates that steep, parabolic temperature gradients are formed initially through the thickness of the section, and that these gradients gradually decrease with time as heat is conducted into the concrete core. In terms of concrete cracking, these temperature gradients are anticipated to have two major effects. First, the steep initial gradients are expected to induce high in-plane tensile stresses in the concrete core that will result in through-thickness cracking. Second, the net increase of the wall temperatures from the baseline operating temperatures are expected to cause significant growth of the overall section. The restraint of this growth at supports, corners, and other structural discontinuities is expected to induce significant out-of-plane moments that may potentially cause flexural cracking. Figure 6-1(b) and 6-1(c) show similar behavior for SC walls in other locations in the CIS.

6.2 Category 1 Stiffness Evaluation

To evaluate the in-plane stresses induced by the initial temperature gradients observed in the heat transfer analysis, a linear thermal stress analysis was conducted in ANSYS that considered the temperature gradient from the original accident thermal design conditions at 1000 seconds on the typical **[ ]** SC wall section. As shown in Figure 6-2, a 3-D model of a wall section was generated that utilized solid elements for the concrete core and shell elements for the steel faceplates. The 1000-second temperatures were then applied to the nodes to create the gradient, and boundary conditions were applied that permitted thermal expansion both in and out of the plane of the wall.

The results of this thermal analysis described in Appendix J are presented in Figure J-7. The figure shows a sectional view of the concrete core in which the variation of vertical in-plane stresses through the thickness of the concrete can be seen. It is observed that the parabolic thermal gradient puts the outer fibers of the concrete core into compression, while the central portion of the concrete thickness is put into tension. The plot contours indicate that the tensile

stresses greatly exceed the concrete tensile strength (taken as $4\sqrt{f'_c}$) over the majority of the section. Thus it can be postulated that in the actual, nonlinear structure, the accident condition temperature gradients would result in through-thickness cracks at intervals along the length and height of the wall.

As illustrated in Appendix D, experiments performed in Japan have demonstrated that the accident thermal condition does cause thermal gradients similar to those predicted by the aforementioned heat transfer analysis, and that the gradients cause the postulated through-thickness cracking in two orthogonal directions. Importantly, these tests also evaluated the reduction in in-plane shear stiffness of SC sections caused by the thermally-induced cracking resulting from exposure to 340°F temperatures similar to those applied to the Category 1 SC walls in the US-APWR. As explained in Appendix D, the results indicated that the tangent in-plane shear stiffness under all applied shear forces was approximately equal to the post-cracking shear stiffness of the composite section, i.e., $K_s + K_{sc}$ as given above by Equation 4-4. Therefore the secant stiffness for the accident thermal condition may be estimated as that of the fully cracked section, as given by Equation 4-10.

Recalling that the out-of-plane flexural stiffness for composite SC walls is taken as that of the cracked-transformed section for all loading conditions, the Category 1 walls are considered cracked for Condition “B” in both shear and flexure. As a result, the cracked damping ratio of **[ ]** discussed in Section 4.1.7 is appropriate for Category 1 under this condition.

6.3 Category 2 Stiffness Evaluation

The in-plane cracking observed in the analysis and experiments for the Category 1 SC walls is also anticipated for the Category 2 walls, which are exposed to the same ambient compartment temperatures during the accident condition. The Category 2 walls will also experience steep parabolic temperature gradients that result in extensive through-thickness concrete cracking. In accordance with ACI 349.1R Section 1.4 (see Reference 22), the effect of this cracking may be addressed in linear elastic analysis models of RC structures by reducing the concrete modulus of elasticity by 50%. This reduction is consistent with that specified in ASCE 43-05 (Reference 1) for cracked in-plane shear stiffness of RC walls. It is also comparable to the reduction in secant stiffness applied to the Category 1 SC walls for this condition, as will be further discussed in Section 8.0.

Flexural stresses induced by thermal loading in the various walls and slabs of the CIS were evaluated using the analysis of the accident thermal condition that was performed in support of the basic design (Reference 9). The intent of this analysis was to assess the stresses induced by restraint of overall thermal growth of the structure. Thus, the average increase in wall and slab temperatures at a given point in time, as given by the heat transfer analysis results specific to each member thickness, were applied to each component of the structure. The point in time considered in this analysis was selected as the point at which the average temperature of the **[ ]** SC walls was maximized, since these walls comprise a majority of the walls in the structure. This was calculated to occur at four days after the postulated pipe rupture, using the thermal gradients given in Figure 6-1.

The results of this analysis were combined with seismic loading and used to evaluate the extent of out-of-plane flexural cracking in the Category 2 walls for Condition “B”. The procedure for this evaluation was similar to that used for Condition “A”; i.e., principal moments due to the Condition “B” loading were compared to the cracking moment for the section (calculated using Equations 5-3 and 5-4). The principal moment contour plot given in Figure J-

10 indicates that, as was expected, moments in excess of the cracking moment occur at the base of the walls and at other discontinuities. The presence of significant cracking for this condition warrants the previously mentioned bounding approach for Category 2 flexural stiffness, wherein the uncracked stiffness is assigned for Condition “A” and the cracked stiffness is assigned for Condition “B”.

Since both cracked in-plane shear stiffness and cracked out-of-plane flexural stiffness are to be assigned for the Category 2 walls, a damping ratio of 7% is considered appropriate for these walls under Condition “B”. This is in accordance with the guidance provided in Regulatory Guide 1.61 for RC walls (Reference 5).

6.4 Category 3 Stiffness Evaluation

The Category 3 primary shield walls are irregular in terms of both their geometry and their exposure to thermal loading. As such, evaluation of the response of these walls to accident thermal loading is not straightforward. In terms of geometry, the walls are arranged in a very rigid, cylindrical shape with nominal thickness that varies from **[ ]**. In addition, the walls have an array of transverse and mid-thickness longitudinal steel plates that divide the concrete into numerous cells, and the walls have four large penetrations for fuel loading instrumentation and equipment. In terms of exposure to thermal loading, Figures 2-6 and 2-7 illustrate that the primary shield walls are encapsulated by the Category 5 massive RC over more than half of their overall height. The Category 5 concrete not only prevents exposure of the outer primary shield face to accident temperatures, but it also restrains any thermal growth of the primary shield walls. Above the Category 5 concrete, the primary shield walls are also restrained on all sides by six different secondary shield walls that frame into the outer primary shield face (see Figure 2-2) and by the RC slabs at elevations **[ ]** . (see Figure 2-6).

Clearly the conditions assumed by the heat transfer analyses discussed for the Category 1 and 2 walls are not applicable to the Category 3 walls. It was assumed that the Category 3 walls would not crack under Condition B loading due to the massive and confined nature of the configuration. This assumption is being validated by a detailed thermal analysis which is being performed with an updated thermal loading profile. However, as described in Reference 23, a parametric study has been performed which has assumed 50% reduction in stiffness for a limited region of the reactor cavity exposed to 450 °F. This study found less than a 1% change in the ISRS at the location of the Reactor Vessel Supports.

6.5 Category 4 Stiffness Evaluation

The Category 4 RC slabs are generally exposed on both faces to the accident thermal temperatures shown in Figure 3-1. As such, their response to thermal loading is assessed using the thermal analysis performed on the CIS for the basic design, as discussed above for the Category 2 walls. Principal moments were calculated for each of the major slabs in the CIS under the 4-day accident thermal condition combined with seismic and dead loads, and then compared to cracking moments calculated using Equations 5-3 and 5-4.

Figure J-11 shows the results of this evaluation for the slab at Elevation **[ ]**. This slab is primarily **[ ]** thickness in certain areas as shown in the Figure J-11. The slab is shown to experience significant thermally induced flexure due to its rigid connection to both the outer RWSP wall and the secondary shielding walls. It is noted from the contours given in the Figure J-11 that the calculated principal moments exceed the cracking

moment in a majority of the slab elements. The presence of significant out-of-plane cracking under this condition justifies use of cracked flexural stiffness and 7% damping for the Category 4 slabs under Condition “B”. This establishes a bounding analysis approach for the primary dynamic response of interest for these slabs, given that uncracked flexural stiffness and 4% damping is to be used for Condition “A”.

6.6 Category 5 Stiffness Evaluation

As shown in Figures 2-6 and 2-7, the massive RC sections in the CIS are founded on the thick R/B complex basemat. As a result, exposure to elevated temperatures following a postulated pipe rupture is generally limited to the top faces and some of the vertical inside faces of these structures. Since all of the Category 5 structures are extremely thick (both horizontally and vertically), this limited exposure to the accident temperatures is not expected to cause significant reductions of stiffness due to concrete cracking. Therefore uncracked stiffness and damping values are considered the best estimate for Category 5 under Condition “B”.

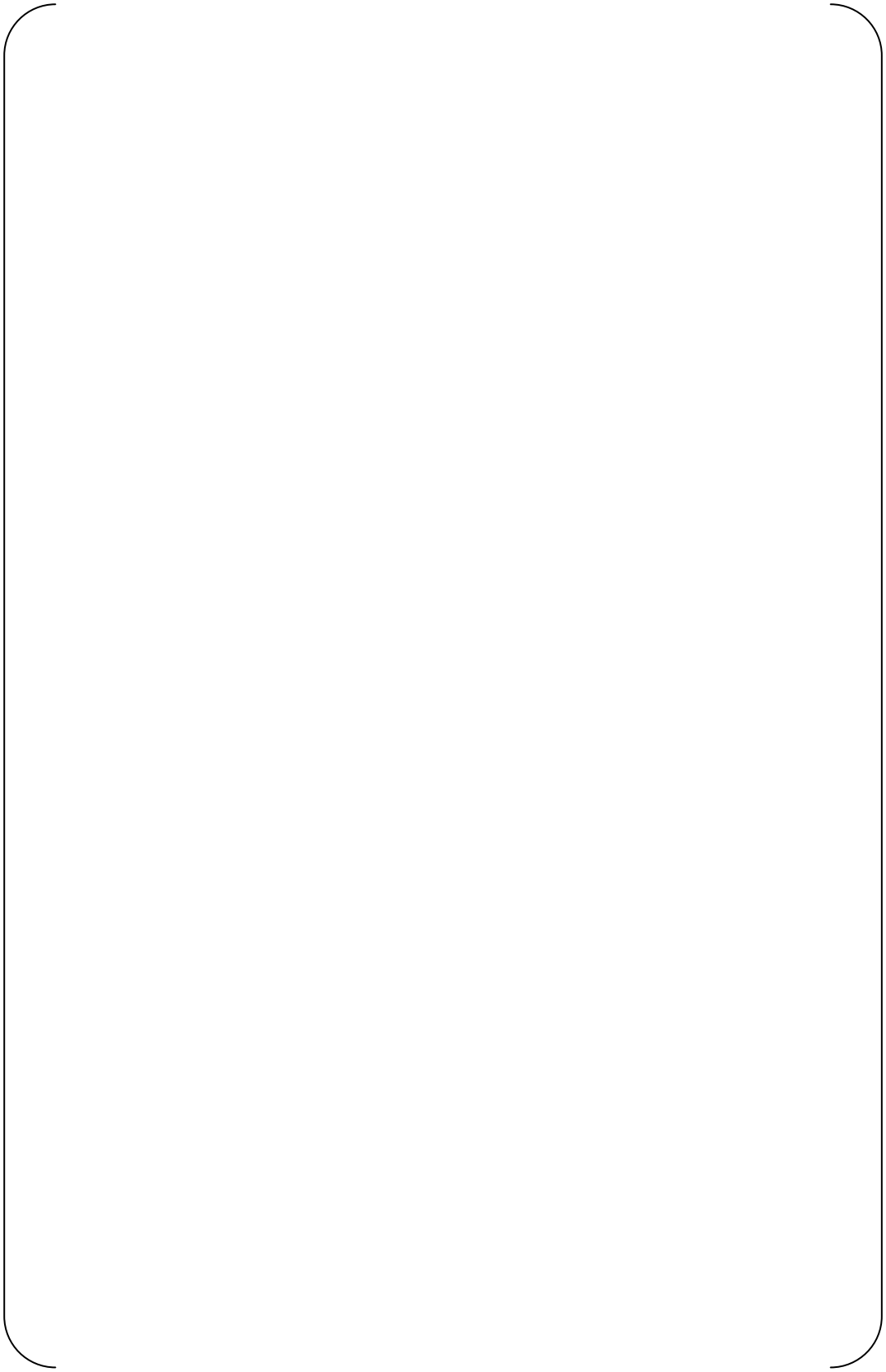

Figure 6-1 Through-Thickness Temperature Gradients Following LOCA

Temperature gradients for SC walls are shown for various timeframes

Figure 6-2 ANSYS Model for Analysis of Accident Thermal Stress in SC Walls

7.0 SUMMARY OF STIFFNESS AND DAMPING VALUES FOR ANALYSIS

A summary of the stiffness and damping values defined above is provided in Table 7-1. For each of the six major structure categories, the table presents the in-plane shear stiffness, out-of-plane flexural stiffness, and damping ratios that have been deemed appropriate for the two analysis cases (Condition “A” and Condition “B”). In general, the table shows that the structure is to be considered as largely uncracked for Condition “A” and cracked for Condition “B”. In several cases, the tabulated values reflect the decision to apply a bounding approach when the assessment of stresses indicated the given structure category was mostly uncracked for Condition “A” and significantly cracked under Condition “B”. Such is the case for the in-plane stiffness of the Category 1 and Category 2 walls and for the flexural stiffness of the Category 4 slabs. However, a bounding analysis approach was not imposed for all structure categories, in the interest of obtaining realistic dynamic responses from both the Condition “A” and Condition “B” analyses. For example, both the Category 3 and Category 5 structures are anticipated to remain mostly uncracked under either loading condition and so a bounding approach is not warranted for these structures. Likewise, the flexural stiffness of the Category 1 SC structures is best approximated by the cracked-transformed stiffness under either loading condition.

In terms of damping, the category-specific damping ratios provided in the table could be applied to each of the various structures in the CIS for each of the two dynamic analyses. However, examination of the individual values given in the table suggests that constant damping ratios may be used. For Condition “A”, 4% damping is identified for all of the structure categories, such that 4% damping is clearly appropriate as an overall, constant damping ratio. For Condition “B”, the individual values range from 4% for the uncracked RC structures to 7% for the cracked RC structures, with **[ ]** assigned to the Category 1 SC walls. Since the Category 1 walls are the primary lateral load resisting members in the structure and their response dominates the amplified range of the overall structure response, 5% damping is deemed an appropriate constant damping ratio for the Condition “B” analyses. In accordance with the guidance given in Regulatory Guide 1.61 (Reference 5), this value is considered appropriate both for generation of forces for structural design and for generation of ISRS for equipment design, since it represents the best estimate of energy dissipation with the cracking levels identified for this condition. It is noted that the **[ ]** value is somewhat conservative for the cracked RC slabs and the cracked Category 2 walls. Damping is not expected to have a significant impact on the seismic response of the relatively rigid structures of Categories 3 and 5, regardless of the values assigned to these structures.

Table 7-1 Summary of CIS Stiffness and Damping Values

8.0 APPLICATION

As mentioned previously, the dynamic response of the CIS will be analyzed using 3-D LEFE models. These models explicitly account for the 3-D geometry of the structure including the extents of each individual wall and slab, using finite elements with linear elastic, isotropic material properties. Thus the geometry of each wall and slab will be modeled using either 3-D solid elements or shell elements. The linear elastic material properties (elastic modulus E and Poisson's ratio ν) and the thickness (t) of these elements will be calibrated to match the effective in-plane shear stiffness and out-of-plane flexural stiffness values given for each structure category in Table 7-1. As stated in the fourth objective in Section 1.1, the calibrated properties will be assigned consistently to the elements of both the ACS SASSI dynamic FE model and the ANSYS detailed design FE model. The primary purpose of this section is to illustrate the manner in which these material and section properties are calculated. In addition, the axial stiffness terms that result from this calibration approach are evaluated, and finally the complete set of stiffness values assigned to the Category 1 SC structures are compared to those recommended in the available nuclear standards for RC structures.

8.1 Calculation of Equivalent Material and Section Properties for Category 1 Walls

The analysis models for both the SSI analysis and the detailed design will use single-layer shell elements with isotropic material properties to model the composite Category 1 SC walls. The procedure presented below is used to calculate equivalent values of section thickness (t') and elastic modulus (E') to match the composite in-plane shear and out-of-plane flexural stiffness values given in Table 7-1.

1. Calculate the in-plane shear stiffness of the section using Equation 4-1 for Condition "A" or Equation 4-10 for Condition "B":

2. For both Conditions "A" and "B", calculate the cracked transformed flexural stiffness for the section using Equation 4-13:

3. Setting $EI = \left(E \cdot t^3\right)/12$, $GA = (E \cdot t)/[2(1+\upsilon)]$ and $\nu = \nu_c$, solve two equations and two unknowns to obtain E' and t' that provide the correct values for GA and EI calculated in steps 1 and 2:

4. Calculate the equivalent density to maintain the correct unit weight with the calculated equivalent thickness:

Appendix I provides the complete set of calculations that follow this procedure for each of the Category 1 wall geometries. The Appendix also provides property calculations for all other structure categories in the CIS for input to the analysis models.

8.2 Discussion of Associated Axial Stiffness

As mentioned in Section 4.1.6, the Category 1 SC wall axial stiffness values implicitly obtained with the *E'* and *t'* values calculated in the manner described above must be evaluated for each of the two loading conditions. The equivalent axial stiffness is calculated per unit width as:

For the upper bound stiffness of Condition "A", the equivalent axial stiffness is evaluated by comparing it to the actual uncracked composite stiffness, which is calculated as follows:

For the lower bound stiffness of Condition "B", the equivalent axial stiffness is compared to the average of cracked and uncracked composite axial stiffnesses, defined previously in Equation 4-16:

These comparisons are performed in the calculations given in Appendix I. The axial stiffness terms calculated with the equivalent material and section properties for Condition "A" are shown to be within 2.6% of the actual uncracked stiffness for all of the Category 1 wall geometries. For Condition "B", the equivalent properties render axial stiffness values that are somewhat softer than the average of the cracked and uncracked composite stiffnesses given by Equation 4-16; the equivalent values range between **[ ]** of the average values. In light of the extensive through-thickness cracking anticipated for Condition "B", these equivalent axial stiffness values provide a rational lower bound for the Category 1 walls. This assessment is further confirmed in view of the axial stiffness values prescribed for RC walls under accident thermal conditions, as discussed below.

8.3 Comparison of SC and RC Stiffness Values

Table 8-1 compares stiffness values for the common **[ ]** SC wall with **[ ]** steel faceplates computed using the equations in Section 4.0 for SC walls with those prescribed by current nuclear standards for RC structures. Specifically, ASCE 43-05 Table 3-1 (Reference 23) is considered for stiffness values of RC structures under seismic loading during normal operations (Condition "A") and ACI 349.1R (Reference 22) is considered for

stiffness reductions due to accident thermal loading (Condition “B”). The various in-plane shear, out-of-plane flexural, and axial stiffness values tabulated for each condition are calculated in Appendix I.

In general, the comparison in Table 8-1 illustrates that the SC-specific formulations for stiffness result in values that are not substantially different from those codified for RC structures. It must be noted, however, that this close comparison is primarily a function of the particular reinforcement ratios selected for the US-APWR SC walls, as the ASCE 43-05 stiffness formulations for RC structures do not explicitly account for reinforcement ratio. Please see Appendix H for further comparison of SC and RC stiffness formulations over a range of reinforcement ratios enveloping those of the US-APWR Category 1 and 2 walls (1.5% to 4.2%).

As discussed in Section 4.0 and the appendices, the Category 1 SC stiffness values in Table 8-1 reflect the behavior of the continuous SC faceplates acting compositely with the concrete core to resist in-plane and out-of-plane loads. This behavior is significantly different than that of concrete reinforced with an orthogonal grid of reinforcement. Nevertheless the favorable comparison of SC and RC stiffness values does indicate that the dynamic response of the US-APWR CIS will be similar to that of a CIS constructed entirely of RC. The reasonably small differences in each stiffness term are readily explained in terms of SC vs. RC behavior.

For Condition “A”, the SC-specific axial and in-plane shear stiffness terms are shown to be **[ ]** larger than those of uncracked RC. Again, this difference is the result of composite resistance to in-plane loads of the steel and concrete in SC construction, while the magnitude of the difference is a function of the selected reinforcement ratio (2.1% in this case). The SC-specific flexural stiffness term for Condition “A” is **[ ]** of that obtained with the RC equation. This difference reflects the fact that SC wall out-of-plane flexural stiffness is best approximated as the cracked-transformed stiffness, as discussed in Appendix E.

For Condition “B”, the SC-specific stiffness values are compared to those obtained using $0.5E_c$, as recommended in ACI 349.1R Section 1.4 Reference 22 for linear elastic analysis of RC structures with thermally induced cracking. For in-plane shear stiffness and axial stiffness, the SC-specific values are **[ ]** of the cracked stiffness values calculated with the RC equations ($0.5G_cA_g$ and $0.5E_cA_g$, respectively). Once again the values are similar, but the SC-specific values reflect the larger in-plane stiffness reduction anticipated for the extensive cracking caused by accident thermal loading, which has been experimentally verified (see Appendix D.) While it is acknowledged that the SC-specific axial stiffness value is likely too soft for portions of walls in compression during seismic loading, it is nevertheless considered a rational lower bound case for use in linear elastic analyses. Any differences in dynamic response due to higher axial stiffness will be captured with the uncracked axial stiffness assigned for Condition “A”. The SC-specific out-of-plane flexural stiffness for this condition is somewhat higher than the value computed for RC, which simply reflects the composite cracked-transformed flexural stiffness for the particular reinforcement ratios used in the US-APWR CIS.

Table 8-1 Comparison of SC and RC Stiffness Values

Stiffness values for the common 48"-thick SC wall section are computed using the SC-specific equations in Section 4.0 and the RC equations given in ASCE 43-05 (Reference 1) for Condition “A” and ACI 349.1R (Reference 22) for Condition “B”.

9.0 SUMMARY

An accurate dynamic analysis can be performed with a linear elastic model only if the model uses the best possible estimation of the effective elastic constants. To this end, stiffness values for each of the structure categories in the CIS have been calculated based on the formulations outlined in Section 4.0, and in consideration of the extent of concrete cracking caused by seismic and accident thermal loading. Two sets of stiffness and damping values have been calculated that capture the potential range of stresses and associated cracking levels in each structure category.

The seismic and thermal load basis for the basic design has been revised since the ranges of stresses were evaluated in accordance with Reference 9. These input changes have been evaluated and it is assumed that they will not have a significant impact to the stiffness and damping conclusions presented in this TeR. The basic analysis is being revised based on the current seismic and thermal load input to confirm the assumption of no impact to this TeR.

It has been shown that both sets of stiffness values obtained with formulations specific to the composite behavior of the Category 1 SC walls are reasonably close to those of RC walls. The manner in which the two sets of stiffness values are applied to the linear elastic models for SSI analysis and detailed structural design has been illustrated. Two corresponding sets of analyses will be conducted in both ACS SASSI and ANSYS to complete Tasks 1-A and 1-B (as described in Reference 3), respectively, in the overall CIS design and validation plan. The enveloped results from these analyses will provide a conservative assessment of the potential range of demands for which the CIS structures and equipment must be designed.

10.0 REFERENCES

1. American Society of Civil Engineers, *"Seismic Design Criteria for Structures, Systems, and Components in Nuclear Facilities,"* ASCE 43-05, May 2005.
2. Mitsubishi Heavy Industries, Ltd., *"Containment Internal Structure Design and Validation Methodology,"* MUAP-11013, Revision 2, February 2013.
3. Mitsubishi Heavy Industries, Ltd., *"Soil-Structure Interaction Analyses and Results for the US-APWR Standard Plant,"* MUAP-10006, Revision 3, November 2012.
4. Mitsubishi Heavy Industries, Ltd., *"Research Achievements of SC Structure and Strength Evaluation of US-APWR SC Structure Based on 1/10th Scale Test Results,"* MUAP-11005, Revision 1, December 2012.
5. U.S. Nuclear Regulatory Commission, *"Damping Values for Seismic Design of Nuclear Power Plants,"* Regulatory Guide 1.61, Revision 1, March 2007.
6. U.S. Nuclear Regulatory Commission, *"Safety-Related Concrete Structures for Nuclear Power Plants (Other Than Reactor Vessels and Containments),"* Regulatory Guide 1.142, Revision 2, November 2001.
7. American Concrete Institute*, "Code Requirements for Nuclear Safety-Related Concrete Structures,"* ACI 349-97, 1997.
8. American Concrete Institute*, "Code Requirements for Nuclear Safety-Related Concrete Structures,"* ACI 349-06, November 2006.
9. URS Corporation, *"Basic Analysis and Design of CIS,"* Calculation CIS-13-05-230-004, Revision 0, March 2011.
10. U.S. Nuclear Regulatory Commission, *"Seismic Design Classification,"* Regulatory Guide 1.29, Revision 4, March 2007.
11. URS Corporation, *"R/B Standard Design SSI Analysis,"* Calculation RB-13-05-113-002, Revision 1, June 2010.
12. Mitsubishi Heavy Industries, Ltd*., "Design Condition for Thermal Analysis of Reactor Building and PCCV,"* N0-EHB0014, Revision 7, February 2013.
13. Ozaki, M., et al., *"Study on Steel Plate Reinforced Concrete Panels Subjected to Cyclic In-Plane Shear,"* Nuclear Engineering and Design, Volume 228, 2004.
14. Sozen, M. and Moehle, J., *"Stiffness of Reinforced Concrete Walls Resisting In-Plane Shear,"* TR-102731, Electric Power Research Institute, August 1993.
15. Lee, M.J., et al., *"In-Plane Shear Behavior of Composite Steel Concrete Walls,"* 5th International Symposium on Steel Structures, March 2009.
16. Kennedy, R.P., et al., *"Engineering Characterization of Ground Motion—Task 1: Effects of Characteristics of Free-Field Motion on Structural Response,"* NUREG/CR-3805, US Nuclear Regulatory Commission, May 1984.
17. Kennedy, R.P., et al., *"Relationship Between Effective Linear Stiffness and Secant Stiffness for Pinched In-Plane Shear Behavior of Shear Walls,"* March 2011.
18. Mitsubishi Heavy Industries, Ltd., *"Damping Ratio of SC Structure,"* MUAP-10002, Revision 0, March 2010.
19. Akiyama, H. et al., *"1/10th Scale Model Test of Inner Concrete Structure Composed of Concrete Filled Steel Bearing Wall,"* 10th International Conference on Structural Mechanics in Reactor Technology (SMiRT10), 1989.
20. Akita, S., et al., *"A Study on the Structural Performance of SC Thick Walls,"* Annual Conference of Architectural Institute of Japan, 2003.

21. U.S. Nuclear Regulatory Commission, *"Combining Modal Responses and Spatial Components in Seismic Response Analyses,"* Regulatory Guide 1.92, Revision 2, July 2006.
22. American Concrete Institute*, "Reinforced Concrete Design for Thermal Effects on Nuclear Power Plant Structures,"* ACI 349.1R-07, May 2007.
23. URS Corporation, *"Impact on CIS Dynamic Response Due to Changes in Accident Thermal Loading,"* Calculation SPS-13-05-100-001, Revision 0, February 2013.

APPENDICES LIST OF FIGURES

APPENDICES LIST OF TABLES

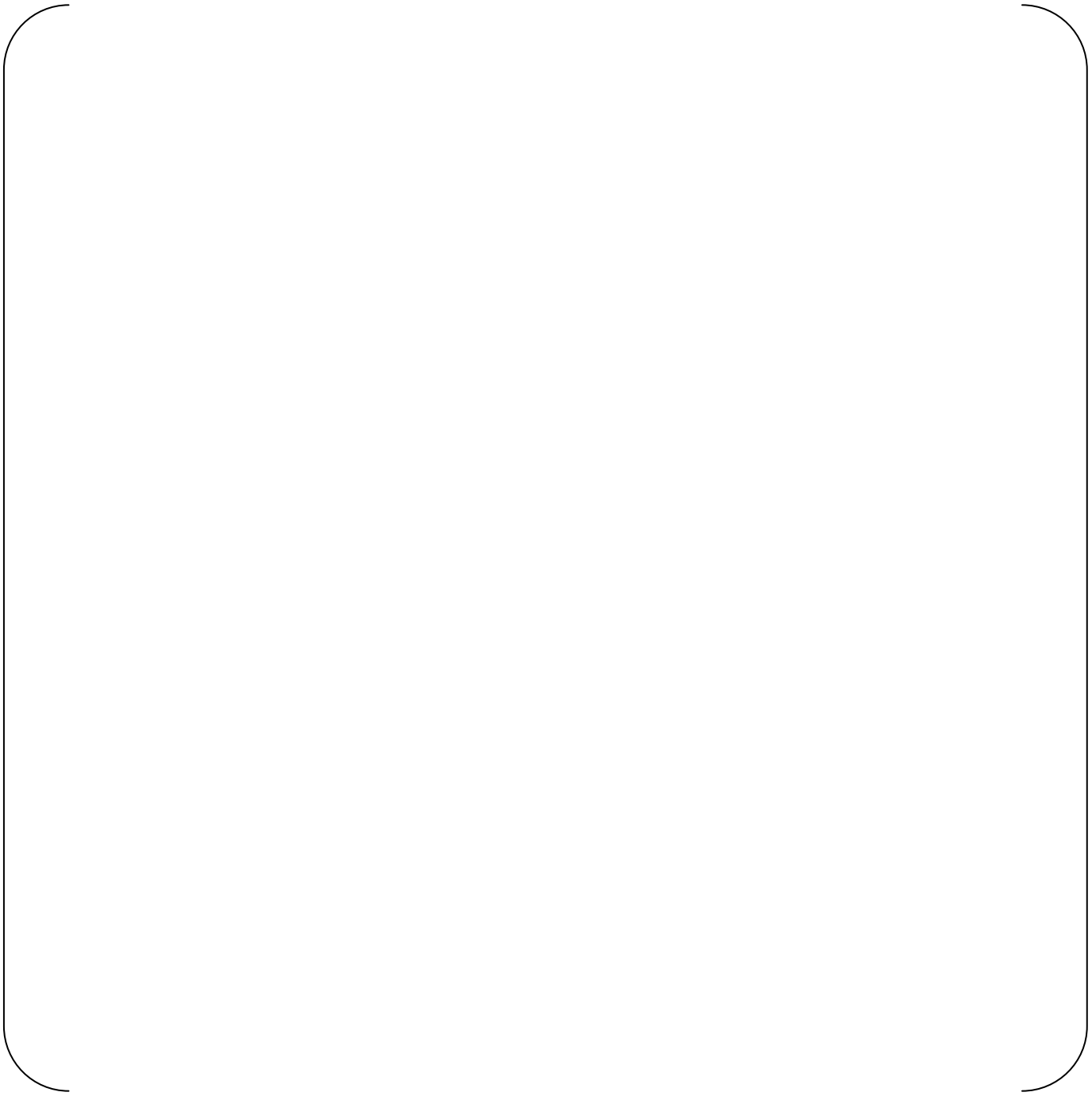

URS

CALCULATION

CALC. BY: DJW DATE : 2-28-12

CHKD. BY: RCJ DATE : 4-25-12

PROJECT TITLE: US-APWR

SUBJECT/FEATURE: MUAP-11018 Appendix G: Effects of Stainless Steel Cladding on SC Stiffness

URS

CALCULATION

CALC. BY: DJW DATE : 2-28-12

CHKD. BY: RCJ DATE : 4-25-12

PROJECT TITLE: US-APWR

SUBJECT/FEATURE: MUAP-11018 Appendix G: Effects of Stainless Steel Cladding on SC Stiffness

URS

CALCULATION

CALC. BY: DJW DATE : 2-28-12

CHKD. BY: RCJ DATE : 4-25-12

PROJECT TITLE: US-APWR

SUBJECT/FEATURE: MUAP-11018 Appendix G: Effects of Stainless Steel Cladding on SC Stiffness

URS

CALCULATION

CALC. BY: DJW DATE : 2-28-12

CHKD. BY: RCJ DATE : 4-25-12

PROJECT TITLE: US-APWR

SUBJECT/FEATURE: MUAP-11018 Appendix G: Effects of Stainless Steel Cladding on SC Stiffness

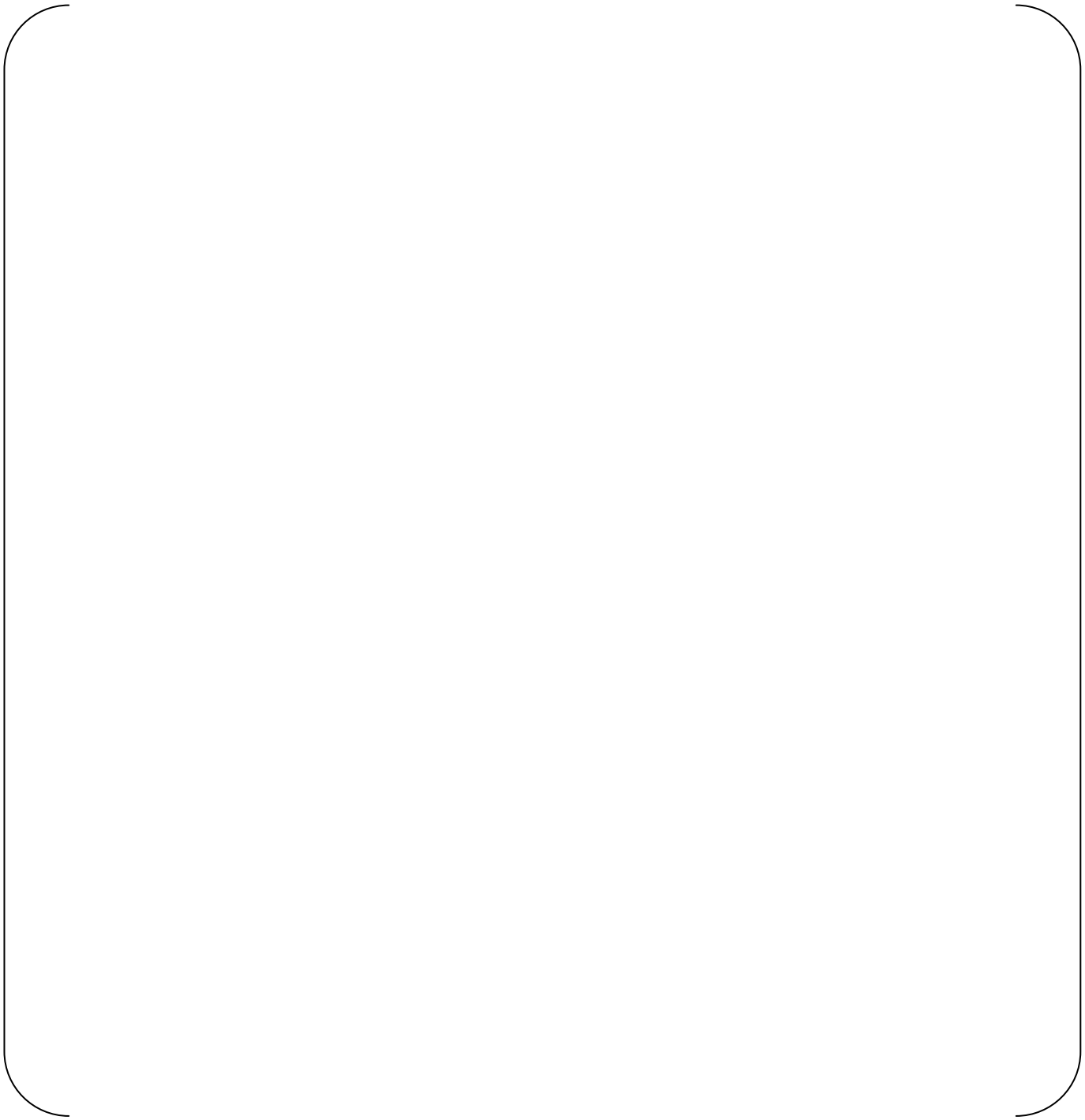

URS

CALCULATION

CALC. BY: DJW DATE : 10-16-12

CHKD. BY: EJB DATE : 10-17-12

PROJECT TITLE: US-APWR

SUBJECT/FEATURE: MUAP-11018 Appendix H: Comparison of SC and RC Stiffness vs. Reinforcement Ratio

URS

CALCULATION

CALC. BY: DJW DATE : 10-16-12

CHKD. BY: EJB DATE : 10-17-12

PROJECT TITLE: US-APWR

SUBJECT/FEATURE: MUAP-11018 Appendix H: Comparison of SC and RC Stiffness vs. Reinforcement Ratio

URS

CALCULATION

CALC. BY: DJW DATE : 10-16-12

CHKD. BY: EJB DATE : 10-17-12

PROJECT TITLE: US-APWR

SUBJECT/FEATURE: MUAP-11018 Appendix H: Comparison of SC and RC Stiffness vs. Reinforcement Ratio

URS

CALCULATION

CALC. BY: DJW DATE : 10-16-12

CHKD. BY: EJB DATE : 10-17-12

PROJECT TITLE: US-APWR

SUBJECT/FEATURE: MUAP-11018 Appendix H: Comparison of SC and RC Stiffness vs. Reinforcement Ratio

URS

CALCULATION

CALC. BY: DJW DATE : 5-3-11

CHKD. BY: CTB DATE : 5-6-11

PROJECT TITLE: US-APWR

SUBJECT/FEATURE: MUAP-11018 Appendix I: Equivalent Material and Section Properties for Analysis

URS

CALCULATION

CALC. BY: DJW DATE : 5-3-11

CHKD. BY: CTB DATE : 5-6-11

PROJECT TITLE: US-APWR

SUBJECT/FEATURE: MUAP-11018 Appendix I: Equivalent Material and Section Properties for Analysis

URS

CALCULATION

CALC. BY: DJW DATE : 5-3-11

CHKD. BY: CTB DATE : 5-6-11

PROJECT TITLE: US-APWR

SUBJECT/FEATURE: MUAP-11018 Appendix I: Equivalent Material and Section Properties for Analysis

URS

CALCULATION

CALC. BY: DJW DATE : 5-3-11

CHKD. BY: CTB DATE : 5-6-11

PROJECT TITLE: US-APWR

SUBJECT/FEATURE: MUAP-11018 Appendix I: Equivalent Material and Section Properties for Analysis

URS

CALCULATION

CALC. BY: DJW DATE : 5-3-11

CHKD. BY: CTB DATE : 5-6-11

PROJECT TITLE: US-APWR

SUBJECT/FEATURE: MUAP-11018 Appendix I: Equivalent Material and Section Properties for Analysis

URS

CALCULATION

CALC. BY: DJW DATE : 5-3-11

CHKD. BY: CTB DATE : 5-6-11

PROJECT TITLE: US-APWR

SUBJECT/FEATURE: MUAP-11018 Appendix I: Equivalent Material and Section Properties for Analysis

URS

CALCULATION

CALC. BY: DJW DATE : 5-3-11

CHKD. BY: CTB DATE : 5-6-11

PROJECT TITLE: US-APWR

SUBJECT/FEATURE: MUAP-11018 Appendix I: Equivalent Material and Section Properties for Analysis

URS

CALCULATION

CALC. BY: DJW DATE : 5-3-11

CHKD. BY: CTB DATE : 5-6-11

PROJECT TITLE: US-APWR

SUBJECT/FEATURE: MUAP-11018 Appendix I: Equivalent Material and Section Properties for Analysis

URS

CALCULATION

CALC. BY: DJW DATE : 5-3-11

CHKD. BY: CTB DATE : 5-6-11

PROJECT TITLE: US-APWR

SUBJECT/FEATURE: MUAP-11018 Appendix I: Equivalent Material and Section Properties for Analysis

URS

CALCULATION

CALC. BY: DJW DATE : 5-3-11

CHKD. BY: CTB DATE : 5-6-11

PROJECT TITLE: US-APWR

SUBJECT/FEATURE: MUAP-11018 Appendix I: Equivalent Material and Section Properties for Analysis

URS

CALCULATION

CALC. BY: DJW DATE : 5-3-11

CHKD. BY: CTB DATE : 5-6-11

PROJECT TITLE: US-APWR

SUBJECT/FEATURE: MUAP-11018 Appendix I: Equivalent Material and Section Properties for Analysis

URS

CALCULATION

CALC. BY: DJW DATE : 5-3-11

CHKD. BY: CTB DATE : 5-6-11

PROJECT TITLE: US-APWR

SUBJECT/FEATURE: MUAP-11018 Appendix I: Equivalent Material and Section Properties for Analysis

URS

CALCULATION

CALC. BY: DJW DATE : 5-3-11

CHKD. BY: CTB DATE : 5-6-11

PROJECT TITLE: US-APWR

SUBJECT/FEATURE: MUAP-11018 Appendix I: Equivalent Material and Section Properties for Analysis

K. APPENDIX K: REFERENCES FOR APPENDICES

K-1 Booth, P.N., Varma, A.H., Malushte, S., and Johnson, W. (2007). “Experimental Behavior of Composite Sandwich Walls for Nuclear Facilities,” *Proceedings of the Annual Structural Mechanics in Reactor Technology Conference*, in press, IASMIRT, North Carolina State University, Rayleigh, NC, 10 pp.

K-2 Ozaki, M., Akita, S., Takeuchi, M., Oosuga, H., Nakayama, T., and Niwa, H., (2000). "Experimental Study on Steel-plate-reinforced Concrete Structure Part 41: Heating Tests (Outline of Experimental Program and Results), Annual Conference of Architectural Institute of Japan, 2000, Part 41-43, pp. 1127-1132

K-3 Ozaki, M., Akita, S., Oosuga, H., Nakayama, T., Adachi, N. (2004). "Study on Steel Plate Reinforced Concrete Panels Subjected to Cyclic In-Plane Shear." Nuclear Engineering and Design, Vol. 228, pp. 225-244.

K-4 Varma, A.H., Malushte, S.R., Sener, K.C., and Booth, P.N. (2009). "Analysis and Design of Modular Composite Walls for Combined Thermal and Mechanical Loading." *Proceedings of the Annual Structural Mechanics in Reactor Technology Conference*, Division TS 6-x.y, Paper 1820, Espoo, Finland, Aug. 9-14, 2009.